

1 Leveraging USArray and Regional Networks to Characterize Natural and Mining Seismicity at  
2 the Intersection of the Grenville and Appalachian Provinces

3 Aubreya Adams<sup>\*1</sup>, Yinuo Jin<sup>1</sup>, Monica Dimas<sup>1</sup>, and Isabel Dove<sup>1,2</sup>

4 \* Corresponding author

5 1 Colgate University

6 2 Now at University of Rhode Island, Graduate School of Oceanography

7

8 Abstract

9 Upstate New York and surrounding regions typically experience low levels of small-magnitude  
10 seismicity, yet several damaging earthquakes have occurred in the region during the past 50  
11 years. Paleoseismic evidence also suggests larger magnitude events occurred in this region in  
12 recent geologic history. This region has undergone numerous mountain-building events,  
13 resulting in complex and overprinting crustal structures that are not always reflected in surficial  
14 geology. The history of damaging earthquakes and complex geology in the region highlight the  
15 importance of characterizing the spatial distribution of seismicity and implications for seismic  
16 hazards. Efforts to delineate regions of higher seismicity face the challenge of differentiating  
17 the typically small-magnitude earthquakes from events generated by the robust mining industry  
18 throughout the region. This study uses a combination of public seismic data and data from three  
19 new seismic stations in the Adirondack Mountains to locate both earthquakes and mining events  
20 in the regions surrounding the Adirondack Mountains between 2013-2017, building upon and  
21 refining existing catalogs. Locations are determined based on manually picked P and S wave  
22 arrival times using a two-step relocation process in Antelope and Hypoinverse and two regional  
23 velocity models. All events were manually quality checked and categorized as natural seismicity

24 or mining events based on waveform characteristics, origin times, and distance from known  
25 mines. We report locations of 107 earthquakes and 178 mining events. Mining events appear  
26 primarily, although not exclusively, associated with limestone mines. Most of the earthquakes  
27 are located within three seismic zones: the Western Quebec Seismic Zone, near the boundary  
28 between the Grenville and Appalachian Provinces, and in a swath extending WNW from the  
29 North Hudson Valley. Notably, the swath of seismicity extending WNW from the North Hudson  
30 Valley does not follow trends of nearby surficial structures, illustrating the complexity of crustal  
31 structures and seismic hazards in the study region.

32

### 33 1.0 Introduction

34 Upstate New York and the surrounding regions have a complex geologic history consisting of  
35 multiple overprinting tectonic events, which are reflected in the geology and seismicity of the  
36 region (Figure 1). Upstate New York is dominated by Grenville-age (approx. 1.3-1.0 BYA)  
37 basement rocks, which are exposed at the surface in the Adirondack Mountains in the northern  
38 portion of the state. To the east, the suture between the Grenville and Taconic Provinces roughly  
39 parallels the boundary between New York and New England but extends westward into New  
40 York south of the Adirondack Mountains near the southern portion of our study area. East of the  
41 Grenville-Taconic suture, a complex series of terrains show overprinting of later Appalachian  
42 orogenies and the subsequent break-up of Pangea. Passing over the Great Meteor Hot Spot  
43 during the Mesozoic further influenced the region, possibly leading to the anomalous uplift of  
44 the Adirondack Mountains (Eby, 1984; Heaman and Kjarsgaard, 2000; Zartman, 1977). Surficial  
45 features created by these tectonic events have been mapped by numerous studies (e.g. Jacobi,

46 2002; Fakundiny, 2004; Regan et al., 2019), but how the structure and geometry of these  
47 boundaries are manifested at deep crustal depths remains poorly understood.

48

49 This region is seismically quiescent compared to many other regions of the contiguous United  
50 States, yet the region has experienced several damaging earthquakes within the past fifty years,  
51 including the 1983 Goodnow and the 2002 Au Sable Forks earthquakes. Furthermore, some  
52 studies suggest the possibility of large magnitude earthquakes (greater than magnitude 7.0)  
53 within the past 7500 years (e.g. Aylsworth et al., 2000; Jacobi and Ebel, 2019). This potential  
54 for seismic hazards highlights the importance of carefully studying intraplate earthquakes. The  
55 task of cataloging earthquakes is, however, complicated by the presence of an active mining  
56 industry in this region, producing mining blasts that must be differentiated from small magnitude  
57 naturally occurring earthquakes.

58

59 The primary goals of this study are to use manual examination of waveforms and a multi-step  
60 relocation algorithm to (a) determine the best characteristics for differentiating mining events  
61 from natural seismicity within the region and (b) develop a catalog of high-quality earthquake  
62 locations that builds upon existing public catalogs by incorporating manual arrival picking and  
63 extensive quality checks, to characterize the natural seismicity of the regions surrounding upstate  
64 New York and the relationship between modern seismicity and ancient tectonic terrains.

65

66 2.0 Geologic Overview

67 The northeastern United States is characterized by a series of westward aging terrains accreted  
68 onto the central cratonic nucleus of North America. Within our study area, the deep crystalline

69 basement consists of Proterozoic Grenville rocks in the west and more recent Paleozoic  
70 Appalachian Provinces to the east, especially those associated with the Taconic Orogeny. In  
71 most locations within the US, and in much of our study region, Grenville rocks are overlain by  
72 younger Paleozoic terrains and Quaternary sediments, but Grenville basement rocks outcrop in  
73 eastern Canada and in northern New York within the Adirondack Mountains. Previous studies of  
74 seismicity suggest that earthquakes are concentrated in the northern and east-central portions of  
75 our study region, with records of several moderately-sized earthquakes in the past century and  
76 evidence of large magnitude earthquakes in the past 10,000 years (e.g. Aylsworth et al., 2000;  
77 Jacobi and Ebel, 2019). The existence of a robust and active mining industry throughout the  
78 study region complicates the delineation of patterns in small-magnitude earthquakes.

79

## 80 2.1 The Grenville Province and the Adirondack Mountains

81 The Grenville Province was accreted to the Superior Craton through several pulses of orogenic  
82 events between 1.3 and 1.0 Ga, when Laurentia collided with several allochthonous terrains and  
83 with Amazonia during the formation of the supercontinent Rodinia (e.g. McLelland et al., 1996,  
84 McLelland, 2010, McLelland and Selleck, 2011; Spencer et al., 2015). Grenville terrains extend  
85 from northeastern and eastern Canada, through the northeastern and east-central United States,  
86 terminating in Texas. Surficial exposure of Grenville-aged rocks is most pervasive in the  
87 Canadian provinces of Quebec and Ontario, while throughout much of the eastern United States  
88 Grenville-aged rocks are buried by more recent tectonic terrains or sedimentary sequences.

89 Insights into structures within these buried Grenville terrains come primarily from crustal and  
90 lithospheric-scale geophysical studies (e.g. Yaun et al., 2014; Yang and Gao, 2018; Long et al.,  
91 2019). One notable exception is the southernmost large-scale exposure of Grenville-aged rocks

92 in the Adirondack Mountains of New York state, which is connected to inland exposures in  
93 Canadian provinces by the narrow Frontenac Terrain.

94

95 The Adirondack Mountains are a dome-shaped region where Grenville basement rocks are  
96 anomalously exposed at the surface. The limbs of the Adirondack dome are asymmetrical,  
97 dipping gently beneath younger sediments to the north, west, and southwest, but dipping steeply  
98 to the east and southeast at the Taconic Thrust. The Adirondack Lowlands comprise a small  
99 section of the westernmost Adirondack Mountains, abutting the Frontenac Terrain. This region  
100 consists primarily of metamorphosed shallow marine sediments formed during the accretion of  
101 an allochthonous terrain during the early stages of the Grenville orogeny, approximately 1.2 Ga  
102 (e.g. Carr et al., 2000; Peck et al., 2013) and is part of the larger Central Metasedimentary Belt  
103 (CMB) that extends throughout the Grenville Province (McLelland et al., 1996). The western  
104 Lowlands are separated from the eastern Adirondack Highlands by the Carthage-Colton  
105 Mylonite Zone (CCMZ), a northeast trending region of high strain exposed in a linear region 110  
106 km long and up to 10 km across (McLelland et al., 1996, McLelland and Isachsen, 1986; Wiener,  
107 1983). The Adirondack Highlands lie east of the CCMZ and comprise the majority of the  
108 Adirondack Mountains. The Highlands were accreted to the Laurentian margin between 1190  
109 and 1140 Ma, with high-grade metamorphism continuing during the accretion of Amazonia  
110 between 1090 and 1020 Ma (Rivers and Corrigan, 2000; Rivers, 2008; McLelland et al., 2010).  
111 The Highlands are characterized by high-grade metamorphic rocks primarily consisting of  
112 granulite facies and belong to the Central Granulite Terrain (CGT) of the broader Grenville  
113 Province. The CGT is further intruded by synorogenic anorthosite plutons, likely generated due  
114 to crustal delamination (e.g. McLelland et al., 2010; Regan et al., 2019). Within the Adirondack

115 Highlands, the most notable of these anorthosite plutons is the roughly 3000 km<sup>2</sup> Marcy Massif,  
116 which dominates a region of both high elevation and high relief in the northeastern Adirondacks,  
117 commonly termed the High Peaks Region.

118

119 Exposure of Grenville rocks within the Adirondack Mountains is anomalous, created by the  
120 asymmetrical domal uplift of the region while contiguous terrains to the north and south are  
121 buried under younger sediments or overthrust by Appalachian provinces. Uplift of the  
122 Adirondack Mountains relative to surrounding terrains likely began during the Mesozoic (e.g.  
123 Crough, 1981; Roden-Tice et al., 2000) and limited evidence of modern uplift suggests continued  
124 uplift at rates ranging from 1-5 mm/year (e.g Isachsen, 1975; Isachsen, 1992). The correlation of  
125 the Adirondack Lowlands and Highlands to the CMB and CGT of the broader Grenville province  
126 suggest that this uplift does not originate from substantial compositional difference between the  
127 Adirondack provinces and Grenville province to the north and south. This anomalous elevation  
128 of the Adirondack Mountains is instead primarily attributed to heating and dynamic uplift by the  
129 Great Meteor Hot Spot, which passed under the region during the Cretaceous (Eby, 1984;  
130 Heaman and Kjarsgaard, 2000; Zartman, 1977). This mechanism for uplift is supported by  
131 recent tomographic evidence for low velocities in the upper mantle (e.g. Levin et al., 2000; Yang  
132 and Gao, 2018). Yang and Gao (2018) found evidence of a low velocity region near the Moho  
133 directly beneath the Adirondack Mountains, which is connected to a broader northeast-trending  
134 low velocity region at approximately 70-85 km depth. They suggest that these tomographic  
135 findings and the anomalous topography of the Adirondack Mountains are best explained by a  
136 localized upwelling of the asthenosphere formed by a combination of edge-convection along the  
137 Laurentian margin and heating by the Great Meteor Hot Spot.

138

139 2.2 Appalachian Provinces

140 East and south of the Grenville-age Adirondack Mountains, southeastern New York and most of  
141 the southern New England states are characterized by the Taconic and Acadian provinces formed  
142 during the accretion of volcanic arcs during the first two phases of the Appalachian Orogeny, and  
143 consist primarily of metamorphosed sedimentary and volcanic rocks. The Grenville and  
144 Appalachian terrains are separated by the north-south trending Taconic Thrust. The Taconic  
145 Thrust dips steeply to east along the border with the Adirondack Mountains, reaching depths of  
146 20 km (Figure 1; Musacchio et al., 1997). To the east of the Taconic suture near the edge of our  
147 study region, a series of narrow N-S trending terrains follow, reflecting a complex history of the  
148 accretion of the Acadian terrain, subsequent metamorphism during the Alleghenian orogeny, and  
149 rifting during the break-up of Pangea.

150

151 Further south, near the Hudson Valley, the boundary between Grenville and Taconic basement  
152 rocks shifts to the west and the steeply dipping Champlain Thrust transitions in southeastern  
153 New York to a broad region in which the Taconic Province overthrusts older Grenville rocks. A  
154 sequence of flysch deposits generated during the Taconic orogeny separates the Grenville and  
155 Taconic Provinces in a narrow region east of the Adirondacks, but broadens to cover much of the  
156 Hudson Valley in the south, corresponding to the overthrust of the Taconic Province in this  
157 region (Bosworth and Vollmer, 1981).

158

159 2.3 Previous Seismicity Studies

160 The Grenville and Appalachian terrains in the northeastern US are characterized by low-to-  
161 moderate levels of intraplate seismicity, which have included several damaging earthquakes  
162 within the past century. Within our study region, seismicity is concentrated in several subregions,  
163 suggesting the importance of preexisting structures in controlling intraplate seismicity. Several  
164 studies have noted spatial correlation between areas of high seismic activity to gravity highs (e.g.  
165 Fakundiny, 2004; Revetta, 2004). Fakundiny (2004) further linked basement geology, patterns  
166 and orientations of fractures and lineaments, and stress conditions with broad patterns in  
167 seismicity to suggest the presence of several independent megablocks within New York and  
168 surrounding regions with different susceptibility to seismic activity. Regions exhibiting the  
169 highest seismic risk correspond to the Western Quebec Seismic Zone (WQSZ) in the border  
170 regions between New York and Quebec, the Highlands and High Peaks regions of the  
171 Adirondack Mountains, and along the Taconic suture through the Hudson Highlands (Fakundiny,  
172 2004).

173

174 During the past century, several moderate-size earthquakes (magnitude  $\geq 4.5$ ) have occurred  
175 within the study region. Table 1 shows origin parameters for 6 such earthquakes listed in the  
176 ANSS catalog (U.S. Geological Survey, 2017). Other sources based on catalogs of individual  
177 networks or compilations of multiple studies indicate similar numbers of moderate-sized events  
178 (e.g. Seeber et al., 2002; Pierre and Lamontagne, 2004). Of the events listed in these historical  
179 catalogs, the most significant in terms of magnitude and damage are the 2002 Au Sable Forks  
180 earthquake and the 1983 Newcombe earthquake. Both earthquakes showed compressional  
181 motion on N-S trending west-ward dipping faults that parallel the Taconic thrust (Seeber and  
182 Armbruster, 1986; Nabelek and Suarez, 1989; Seeber et al., 2002). Both earthquakes suggest

183 reactivation of faults associated with the break-up of Rodinia and the later closure of the Iapetus  
184 ocean during the Taconic Orogeny (Seeber et al., 2002). While the populations of nearby  
185 settlements are small, considerable damage to public infrastructure and private property  
186 occurred. Pierre and Lamontagne (2004) catalog damage from the Au Sable Forks earthquake,  
187 including damage to homes, roads, bridges, and to power and water systems, totaling \$10 million  
188 in damages across six counties. In the northern portions of our study area, paleoseismic studies  
189 give evidence for two large ( $M > 7$ ) earthquakes within the WQSZ occurring 4550 and 7060 Ma  
190 (Aylsworth et al., 2000; Brooks, 2013). The occurrence of damaging earthquakes during the past  
191 century, together with evidence of large earthquakes in recent geologic history, highlight the  
192 importance of characterizing seismicity and seismic hazards within the region.

193

#### 194 2.4 Mining

195 The study region is home to an active mining industry, consisting primarily of surficial mines, or  
196 quarries. In New York alone, there are currently 1,783 mines with active permits and 3,105  
197 mines with reclaimed mining permits (NY DEC), while in Vermont, 33 mines are classified as  
198 active and an additional 148 mines are classified as intermittently active (Vermont DEC). In  
199 both states, which make up the bulk of our study region, active mines consist primarily of sand  
200 and gravel or limestone quarries, with numerous other commodities mined to lesser degrees.  
201 For example, New York mines are also an important source of salt, wollastonite, talc, garnet and  
202 zinc.

203

204 The prominent role of mining within the study region poses a challenge for differentiating small  
205 magnitude earthquakes from man-made events produced by mining activities. Previous studies

206 in other regions with active mining industries have used a combination of waveform properties  
207 and proximity to known mines to distinguish earthquakes from mine blasts. Waveform  
208 characteristics that may be diagnostic of mine blasts include emergent P-wave arrivals, multiple  
209 P-wave arrivals, emergent or ambiguous S-wave arrivals and prominence of low frequency  
210 signals at most stations, as well as long cudas (>25s) for stations less than 1° from the event  
211 source location (Stump et al., 2002; Lockridge et al., 2012; Homman, 2015).

212

213 3.0 Data and Methodology

214 3.1 Data

215 This study leverages broadband data from several public and private networks in the US and  
216 Canada from 2013-2017 (Figure 2). Most notably, the USArray Transportable Array (TA) was  
217 installed in the study region between 2012-2015 and included a total of 49 broadband stations  
218 during the first year of our study. Following the removal of the TA from the contiguous United  
219 States, 13 former TA stations were adopted into regional networks. The Lamont-Dougherty  
220 Cooperative Seismic Network (LDCSN; network LD) operated a total of 23 stations in New  
221 York and in New England within our study area, although not all stations were operating  
222 simultaneously.

223

224 Existing publicly available data from these and other sources were supplemented by three  
225 additional stations (network YM; red circles in Figure 2) installed and operated by the authors in  
226 the High Peaks region of the Adirondack Mountains from 2015-2017. This region was selected  
227 because of its proximity to notable historic earthquakes, and due to the greater than average  
228 interstation distances for TA stations in that region, which resulted from limited infrastructure

229 and accessibility. Stations in the YM network were instrumented by Meridian Compact Posthole  
230 Seismometers with 120 s corner frequencies. To accommodate data collection in these more  
231 remote regions, YM stations were solar powered, and data were stored locally on disks and were  
232 collected several times during each year.

233

### 234 3.2 Arrival Detections and Initial Locations

235 Event locations were determined through an iterative process (see Figure A1 in Appendix).  
236 Initial location was based on automated detection of P- and S-wave arrivals using the ratio of  
237 short-term average amplitudes to long-term average amplitudes (STA/LTA) in Antelope.  
238 Amplitude ratios were considered for all three components and at several frequency bands (0.5-  
239 1.2 Hz, 0.8-3 Hz, 2-6 Hz, 3-10 Hz, and 3 Hz high pass). In cases with at least 4 detected arrivals  
240 within a 500 s window, a preliminary automatic location was made using an IASP91 velocity  
241 model (Kennet and Engdahl, 1991).

242

243 All events correlating to those listed in the Advance National Seismic System Comprehensive  
244 Catalog (ANSS) were selected for further manual examination (U.S. Geological Survey, 2017).  
245 Additionally, events with sufficient automatically detected arrivals, but that were not listed in the  
246 ANSS catalog, were selected for manual quality check and more detailed relocation. For  
247 earthquakes occurring during the deployment of the TA, a minimum of 15 automatic detections  
248 were required for events not listed in the ANSS catalog. Following the demobilization of the  
249 TA, many former TA stations were adopted into regional networks, but others were removed and  
250 not replaced, resulting in fewer possible detections during the later portion of our study. To

251 accommodate this smaller number of stations, the required number of automatic detections was  
252 decreased to a minimum of 11 following the removal of the TA network.

253

254 During manual quality check, all three components were examined. Automatic arrival picks  
255 were adjusted when necessary, duplicate detections were removed, and additional arrivals were  
256 marked. Only arrivals that could be picked with an uncertainty less than 0.5 seconds (P-wave) or  
257 1 second (S-wave) were kept. Whenever possible, arrivals were picked based exclusively on  
258 unfiltered seismograms, but occasionally minimum phase bandpass butterworth filters within the  
259 range of 0.3-10 Hz were also examined for records with low signal-to-noise ratios. Following  
260 this manual quality check and addition of new arrivals, an initial relocation was performed using  
261 dbgenloc in Antelope (Pavlis et al., 2004) and a 1D regional velocity model representing  
262 structure in the Grenville province (Viegas et al., 2011; Figure 3).

263

### 264 3.3 Relocation

265 Following an initial relocation of events within Antelope, more refined locations were  
266 determined using Hypoinverse (Klein, 2002), incorporating separate velocity models for the  
267 Grenville and Appalachian portions of our study region. We used 1D average P-wave velocity  
268 models for each of the two regions determined by propagation of waves from the 2002 Au Sable  
269 Forks earthquake, which corresponds to the travel paths for earthquakes within the central  
270 portion of our study region (Viegas et al., 2011; Figure 3). A P-S ratio of 1.76 was used for both  
271 models based on results from Viegas et al. (2011). Each station in the study was assigned to one  
272 of the two velocity models based on location (see symbol outlines in Figure 2).

273

274 During relocation in Hypoinverse, source locations were refined iteratively until either the  
275 change in hypocenter location between iterations fell beneath 0.04 km or the RMS residual of  
276 arrival times fell beneath 0.001 s, up to a maximum of 30 iterations. Beginning with the fourth  
277 iteration, weights were applied to all observations based on RMS residuals and distance.  
278 Observations with RMS residuals greater than 0.3 s were given zero weight, tapering to full  
279 weight for arrivals with an RMS residual of 0 s. Typical interstation distances within our study  
280 region were approximately 75 km. To balance these large interstation distances with the  
281 decreasing constraint given by distant stations, observations were weighted by distance. Full  
282 weight was given to stations within 100 km with a cosine taper to zero-weight at distances  
283 greater than or equal to 800 km. Preliminary latitudes and longitudes from Antelope were used  
284 for starting locations, and several initial trial depths at 5 km intervals between 0-20 km were  
285 tested. Most events showed little sensitivity to starting depths, with an average standard  
286 deviation of final depths between trial runs of 1.99 km for earthquakes and 1.02 km for mining  
287 events. Based on the minimal values of depth error, starting depths of 0 km and 15 km were  
288 selected for mining events and earthquakes, respectively. Following iterative relocation in  
289 Hypoinverse, events with a horizontal error greater than 10 km, a vertical error greater than 5  
290 km, or fewer than 5 stations after distance and RMS weighting were rejected.

291

### 292 3.4 Differentiation from Mining Events

293 In an area of active mining, it is necessary to differentiate man-made sources, such as mining  
294 blasts, from earthquakes. We follow the model of previous studies in using waveform  
295 characteristics to manually categorize each event as an earthquake or a mining event described in  
296 previous sections (Stump et al., 2002; Lockridge et al., 2012; Homman, 2015) (Figure 4).

297 Waveform characteristics that were most diagnostic of mining blasts in our catalog included  
298 numerous emergent P-wave arrivals, prominence of low frequency signals at most stations, and  
299 long codas (>25 s) for stations less than 1° from the event. For ambiguous events, distance  
300 between the epicenter and the closest mine was also considered in the classification, as well as  
301 time of day and similarity to times of proximal events showing clear characteristics of a man-  
302 made source.

303

#### 304 4.0 Results and Discussion

305 In addition to 110 earthquakes listed in the ANSS catalog (U.S. Geological Survey, 2017), 188  
306 events were selected for further evaluation based on the number and quality of automated picks,  
307 totaling 298 events. For all selected events, P and S wave arrivals were manually picked, and  
308 pick errors were estimated. These events were initially located in Antelope using a 1D velocity  
309 model for the Grenville Province (Viegas et al., 2011) and were categorized as earthquakes (118)  
310 or mining events (180). Figure 5 shows the location of the events selected for evaluation based  
311 on number of automated picks. Mining events are found primarily along the borders between  
312 tectonic blocks, and depths of mining events from preliminary Antelope locations extend up to  
313 14.81 km with an average depth of 1.68 km and a standard deviation of 2.87 km, demonstrating  
314 that this preliminary location using a single velocity model is insufficient to accurately locate  
315 many mining events. Earthquakes are more broadly distributed across diffuse swaths near the  
316 northern and eastern borders of the Adirondack Mountains, with smaller numbers of events in  
317 western New York and in the Appalachian Provinces. Earthquake depths from Antelope  
318 locations extend to depths of 36.79 km, with an average depth of 7.22 km and a standard  
319 deviation of 7.04 km.

320

321 During relocation using two regional velocity models in Hypoinverse, 13 events with a  
322 horizontal location error greater than 10 km, a vertical location error greater than 5 km, or  
323 recorded on fewer than 5 stations were rejected, resulting in a final count of 107 well-located  
324 earthquakes and 178 well-located mining events. (See Tables A2 and A3 in Appendix for  
325 information on rejection criteria by event.) Figure 6 shows locations of events following  
326 relocation in Hypoinverse. First-order spatial patterns for both types of events are similar to  
327 those from Antelope locations (Figure 5), but some refinements in horizontal locations and  
328 significant differences in depth distribution are observed.

329

330 Mine events in the western portion of the study region show only small changes in location  
331 following relocation using Hypoinverse, however events closer to the Taconic suture are shifted  
332 slightly towards the east and display tighter clustering around known mine locations following  
333 relocation in Hypoinverse. Average lateral location error is 0.54 km. Location of mining events  
334 are strongly, although not exclusively, correlated with limestone mines (NY DEC). Average  
335 depths of mining events decrease significantly, with an average depth and depth error of 0.60 +-  
336 1.65 km. Both changes to source locations likely reflect the inclusion of a second velocity model  
337 for the Appalachian Province that better describes velocities along the paths to stations in the  
338 eastern portion of the study region. The maximum calculated depth for a mining event reached  
339 7.86 km for an event found in the Mohawk Valley region. Several other events in this region  
340 were also located at depths that, even accounting for depth uncertainty, were too deep to  
341 accurately represent the depth of mining activity. These events were carefully reexamined, but  
342 were determined to clearly show waveform characteristics typical of mining events, and had

343 origin times that were similar to proximal mining events. While the excessive depths of these  
344 events could represent complex sources triggered by mine blasts, it is likely that the complex  
345 geology in this area, which is not accurately captured by two regional 1D velocity models, could  
346 lead to overestimation of these depths. This region experienced significant overthrust of  
347 Grenville basement by the Taconic Terrain during the Taconic Orogeny, which likely resulted in  
348 the structures not reflected by either the Grenville or Appalachian models of Viegas et al. (2010).  
349 Furthermore, sedimentary layers from the Catskill Depth reach greater thicknesses in this region  
350 than in the rest of the study region (Faill, 1985), a second spatial variation not captured by 1D  
351 velocity models. While several 3D velocity models exist for the mantle and lower crust in this  
352 region (e.g. Yuan et al., 2014; Yang and Gao, 2018), no such model exists which accurately  
353 captures the upper crust. These findings highlight the need for such a model to better characterize  
354 tectonic provinces at depth within the crust and to allow for better locations of local events.

355

356 Following relocation using Hypoinverse, earthquake hypocentral locations changed little  
357 laterally, and lateral errors were low, averaging 0.57 km. Average depth increased from 7.22 km  
358 prior to relocation and an average depth of 9.62 +- 1.32 km after relocation. Earthquake  
359 locations show a strong correlation to previously existing crustal structures, primarily along the  
360 WQSZ, in the Adirondack Highlands, and along the Taconic suture near the Mohawk Valley. In  
361 the WQSZ and the northern Adirondack Highlands, earthquakes are distributed across a broad  
362 150 km wide swath. In the western WQSZ, earthquakes are primarily confined to the upper 10  
363 km, while in the eastern WQSZ and the northern Adirondack Highlands, earthquakes are deeper.  
364 In this region, few earthquakes have source depths less than 5 km, and most earthquakes have  
365 epicenters at mid-crustal depths of 10-15 km.

366

367 A narrow region of seismicity also extends along the southern and southeastern boundaries of the  
368 Adirondack Mountains. These events extend west-northwest and northwest from the Taconic  
369 Suture near the Upper Hudson Valley into the Mohawk Valley. To the south, these lineations of  
370 earthquakes correlate with a NW-SE trending pre-Taconic shear zone along the northeastern end  
371 of the Scranton Gravity high (Benoit et al., 2014). To the north, the northwest-southeast lineation  
372 extends into the southern Adirondack Mountains towards the center of the CGT, ending south of  
373 the Marcy Massif. These events are located southeast of the 1983 Goodnow Earthquake (see  
374 Figure 1) and follow a trend subparallel to the fault plane of the 1983 Goodnow Earthquake  
375 (Seeber and Armbruster, 1986), fault planes of its aftershocks (Liu et al., 1991), a 2011  
376 earthquake swarm near the North Hudson Valley (Jacobi and Ebel, 2019), and the shear zone  
377 along the northern boundary of the Scranton Gravity High to the south (Benoit et al., 2014).  
378 These WNW-ESE and NW-SE trending features in this region differ from the predominantly  
379 NE-SW and N-S trends of mapped surficial faults through the Adirondack Mountains and  
380 Appalachian Provinces within New York state (e.g. Jacobi, 2002). This area of substantially  
381 different patterns in seismicity suggest the presence of a previously existing crustal structure,  
382 which may not be clearly expressed in surficial features. Such regional variability may carry  
383 important implications for regional seismic hazards, and may lend insights into complex mid-to-  
384 deep crustal structures in this region of the suture between Grenville and Taconic basement  
385 rocks.

386

387 This new catalog of mine events and earthquakes has several differences from the existing  
388 catalog from ANSS contributors (see Tables A4 and A5 in Appendix; U.S. Geological Survey,

389 2017). This study has identified eight earthquakes not listed in the ANSS catalog, located  
390 primarily along the borders of the Adirondack Mountains. Events that are co-listed in this study  
391 and the ANSS catalog differ little in epicentral location, with only four events showing a lateral  
392 shift of greater than 10 km and a minor reduction of 0.03 km in depth error for this study.  
393 Hypocentral depths show an average difference of 3.91 km between this study and the ANSS  
394 catalog, with many source depths in the ANSS catalog fixed at 5 km. This results in a significant  
395 decrease in depth error in this study, with an average depth error reduction of 12.58 km.  
396 Comparisons of the number of stations used for locations varies for individual events, with an  
397 average of 0.75 additional stations used in this study.

398

## 399 5.0 Conclusions

400 This study investigates seismicity in upstate New York and surrounding regions, where a  
401 combination of complex basement geology, limited numbers of earthquakes, and a vigorous  
402 mining industry provide challenges to characterizing seismicity. Using a combination of public  
403 seismic networks and private stations in the High Peaks region of the Adirondack Mountains and  
404 a two-step location process, a total of 285 events were well-located, including 107 earthquakes  
405 and 178 mining events. While a number of waveform and source characteristics were used to  
406 differentiate earthquakes from mining events, those that were most useful in this region were  
407 emergent P-wave arrivals, low frequencies dominating most records, and long cudas (>25 s) for  
408 nearby stations. Approximately two-thirds of events in the study area showed characteristics of  
409 mining blasts and were most frequently associated with limestone mines.

410

411 Most earthquakes within the study region occur in three seismic zones: the WQSZ, the Taconic  
412 Suture, and a region of seismicity extending WNW from the North Hudson Valley. Earthquakes  
413 within the WQSZ are spread across a broad, roughly 150 km wide, region along the St.  
414 Lawrence River Valley and the northernmost Adirondack Mountains, with depths ranging from  
415 primarily upper crust in the west to primarily middle crust in the east. Along the eastern portion  
416 of the study region, earthquakes are less numerous and occur sparsely within the Appalachian  
417 terrains and along surficial expression of the steeply-dipping Taconic Suture.

418

419 In the North Hudson Valley, two regions of seismicity extend NW toward the central CGT and  
420 WNW into the Mohawk Valley. Seismicity extending WNW and NW differ from the dominant  
421 structural trends in our study region, which are predominantly N-S and NE-SW. Similar  
422 orientations within this region have been observed for magnetic lineations, a potential pre-  
423 Taconic shear zone, fault plane solutions, and historical earthquakes. It is notable that this region  
424 also corresponds to the shallowing of the Taconic suture and a transition from a N-S orientation  
425 of the suture to the north to a NE-SW orientation in the south. This suggests significant changes  
426 in crustal structure and stress, and potentially seismic hazards, in this region which are not  
427 clearly reflected in surficial geology.

428

429 Our findings highlight important characteristics of mining events in the study region, enabling  
430 clearer differentiation between mining events and natural seismicity. We find patterns in  
431 earthquake locations supporting known regions of seismicity in the north and eastern portions of  
432 our study region, while also highlighting a region along the Mohawk Valley and the southeastern  
433 Adirondack Mountains where trends in the seismicity add to prior geologic and geophysical

434 evidence for significant spatial changes in crustal structures, not reflected at the surface. Further  
435 study to define variations in velocity structure in this region is critical to providing improved  
436 earthquake locations, to characterize the tectonic history of this region, and to better understand  
437 implications of this spatial variability for seismic hazards.

438

439 Data and Resources:

440 Data were collected by the Global Seismic Network, the USArray Transportable Array, the

441 Lamont-Doherty Cooperative Seismic Network, the Central and Eastern US Network, the

442 Portable Observatories for Lithospheric Analysis and Research Investigating Seismicity, the

443 United States National Seismic Network, the New England Seismic Network, the Southern

444 Ontario Seismic Network, the Canadian National Seismograph Network, and the Colgate

445 Seismic Network. All data are archived at the IRIS Data Management Center. Maps were made

446 using the Generic Mapping Tools version 5.4 ([www.soest.hawaii.edu/gmt](http://www.soest.hawaii.edu/gmt); Wessel and Smith,

447 1998).

448

449 Acknowledgements

450 The authors gratefully acknowledge funding from Colgate University, and advice from Prof.

451 Wong-Young Kim at Lamont-Doherty Earth Observatory.

452

453

- 454 References:
- 455
- 456 Aylsworth JM, Lawrence DE, Guertin J (2000) Did two massiv earthquakes in the Holocene  
457 induce widespread landsliding and near-surface deformation in part of the Ottawa Valley?  
458 *Canada: Geol.*, **28**, 903–906
- 459
- 460 Benoit, M., C. Ebinger, and M. Crampton (2014). Orogenic bending around a rigid Proterozoic  
461 magmatic rift beneath the Central Appalachian Mountains, *Earth and Planetary Science Letters*,  
462 **402** 197-208.
- 463
- 464 Bosworth, W., and F. W. Vollmer (1981). Structures of the Medial Ordovician Flysch of Eastern  
465 New York: Deformation of Synorogenic Deposits in an Overthrust Environment, *The Journal of*  
466 *Geology*, **89:5** 551-568.
- 467
- 468 Brooks, G.R. (2013). A massive sensitive clay landslide, Quyon Valley, southwestern Quebec,  
469 Canada, and evidence for a paleoearthquake triggering mechanism. *Quaternary Research*, **80**,  
470 425–434. doi:10.1016/j.yqres.2013.07.008.
- 471
- 472 Carr, S.D., R.M. Easton, R.A. Jamieson, N.G. Culshaw (2000) Geologic transect across the  
473 Grenville orogen of Ontario and New York. *Can J Earth Sci* **27**, 193–216
- 474
- 475 Crough, S.T. (1981) Mesozoic hotspot epeirogeny in eastern North America. *Geology* **9**, 2–6
- 476

- 477 Eby, G. N. (1984). Geochronology of the Monteregean Hills Alkaline Igneous Province, Quebec.
- 478 *Geology*, **12(8)**, 468–470. [https://doi.org/10.1130/0091-7613\(1984\)12.468-470](https://doi.org/10.1130/0091-7613(1984)12.468-470)
- 479
- 480 Faill, R. (1985). The Acadian orogeny and the Catskill Delta, in *Geological Society of America*
- 481 *Special Paper 201*, 15-37.
- 482
- 483 Fakundiny, R. H. (2004). Delineation of tectonic Provinces of New York state as a component of
- 484 seismic-hazard evaluation, *Northeastern Geology & Environmental Sciences*, **26**, 142-173.
- 485
- 486 Heaman, L. M., & B. A. Kjarsgaard (2000). Timing of eastern North American kimberlite
- 487 magmatism: Continental extension of the Great Meteor hotspot track? *Earth and Planetary*
- 488 *Science Letters*, **178(3–4)**, 253–268. <https://doi.org/10.2183/pjab.71.61>
- 489
- 490 Homman, K.A (2015). Seismicity in Pennsylvania, Master's Thesis, The Pennsylvania State
- 491 University, University Park, PA.
- 492
- 493 Isachsen, Y. W. (1975). Possible evidence for contemporary doming of the Adirondack
- 494 Mountains, New York, and suggested implications for regional tectonics and seismicity.
- 495 *Tectonophysics*, **29(1–4)**, 169–181. [https://doi.org/10.1016/0040-1951\(75\)90142-0](https://doi.org/10.1016/0040-1951(75)90142-0)
- 496
- 497 Isachsen, Y. W. (1992). The Adirondacks: Still rising after all these years, *Natural History*, **5**,
- 498 383-387.
- 499

- 500 Jacobi, R.D., (2002). Basement faults and seismicity in the Appalachian Basin of New York  
501 State. *Tectonophysics*, **353**, 75–113.
- 502
- 503 Jacobi, R. D, and J. E. Ebel (2019) Seismotectonic implications of the Berne earthquake swarms  
504 west-southwest of Albany, New York. *Lithosphere*, **11(5)**, 750–764.  
505 doi: <https://doi.org/10.1130/L1066.1>
- 506
- 507 Kennett, B.L.N. and E.R. Engdahl (1991). Travel times for global earthquake location and phase  
508 association, *Geophysical Journal International*, **105**, 429-465.
- 509
- 510 Klein, F.W. (2002). User's Guide to HYPOINVERSE-2000, a Fortran Program to Solve for  
511 Earthquake Locations and Magnitudes, United Stated Department of the Interior Geological  
512 Survey, Open File Report 02-171.
- 513
- 514 Kumarapeli, P.S. an V.A. Saull (1966) The St. Lawrence valley system: a North American  
515 equivalent of the East African rift valley system. *Can J Earth Sci*, **3**, 639–658
- 516
- 517 Levin, V., W. Menke, & J. Park (2000). No regional anisotropic domains in the northeastern US  
518 Appalachians, *Journal of Geophysical Research*, **105(B8)**, 19,029–19,042.  
519 <https://doi.org/10.1029/2000JB900123>
- 520

- 521 Liu, S., R. Herrmann, J. Xie, and E. Cranswick (1991). Waveform characteristics and focal  
522 mechanism solutions of five aftershocks of the 1983 Goodnow, New York, earthquake by  
523 polarization analysis and waveform modeling, *Seismological Research Letters*, **62**, 123-133.
- 524
- 525 Lockridge, J. S., M. J. Fouch, and J. R. Arrowsmith, (2012). Seismicity Within Arizona during  
526 the Deployment of the EarthScope USArray Transportable Array, *Bulletin of the Seismological  
527 Society of America*, **102(4)**, 1850–1863.
- 528
- 529 Long, M., M.H. Benoit, J.C. Aragon, and S.D. King (2019). Seismic imaging of mid-crustal  
530 structure beneath central and eastern North America: Possibly the elusive Grenville deformation?  
531 *Geology*, **47(4)**, 371-374, <https://doi.org/10.1130/G46077.1>
- 532
- 533 Ma, S., and D. Motazedian (2012). Studies on the June 23, 2010 north Ottawa Mw 5.2  
534 earthquake and vicinity seismicity, *Journal of Seismology*, **16** 513-534, 10.1007/s10950-012-  
535 9294-7.
- 536
- 537 Ma, S. and P. Audet (2014). The 5.2 magnitude earthquake near Ladysmith, Quebec, 17 May  
538 2013: implications for the seismotectonics of the Ottawa-Bonnechere Graben, *Can. J. Earth Sci.*,  
539 **51** 439-451 dx.doi.org/10.1139/cjes-2013-0215.
- 540
- 541 McLlland, J.M., J.S. Daly, and J.M. McLlland, (1996). The Grenville orogenic cycle (ca.  
542 1350–1000 Ma): An Adirondack perspective, *Tectonophysics*, **265**, p. 1–28, doi:10.1016/S0040-  
543 1951(96)00144-8.

- 544
- 545 McLlland, J.M., and B.W. Selleck (2011), Megacrystic Gore Mountain-type garnets in the  
546 Adirondack Highlands: Age, origin, and tectonic implications, *Geosphere*, **7**, p. 1194–1208,  
547 <http://dx.doi.org/10.1130/GES00683.1>.
- 548
- 549 McLlland, J.M., B.W. Selleck, and M.E. Bickford, (2010). Review of the Proterozoic evolution  
550 of the Grenville Province, its Adirondack outlier, and the Mesoproterozoi inliers of the  
551 Appalachians, in Tollo, R.P., et al., eds., *From Rodinia to Pangea: The lithotectonic record of*  
552 *the Appalachian region: Geological Society of America Memoir* **206**, p. 21-49,  
553 doi:10.1130/2010.1206(02).
- 554
- 555 McLlland, J.M. and Y. W. Isachsen (1985) Synthesis of geology of the Adirondack Mountains,  
556 New York, and their tectonic setting within the southwestern Grenville Province, in *The*  
557 *Grenville Province Geological Association of Canada Special Paper*, edited by J.M. Moore, A.  
558 Davidson, and A.J. Baer, **31**, 75-94.
- 559
- 560 Musacchio, G., W. D. Mooney, and J. H. Luetgert (1997). Composition of the crust in the  
561 Grenville and Appalachian Provinces of North America inferred from VP/VS ratios, *Journal of*  
562 *Geophysical Research*, **102(B7)**, 15225-15241.
- 563
- 564 Nabelek, J., and G. Suarez, (1989). The 1983 Goodnow earthquake in the central Adirondacks,  
565 New York: Rupture of a simple, circular crack, *Bulletin of the Seismological Society of America*,  
566 **79**, p. 1762–1777.

- 567
- 568 NY DEC, Downloadable Mining Database, Retrieved from:  
569 <https://www.dec.ny.gov/lands/5374.html>
- 570
- 571 Pavlis, G., F. Vernon, D. Harvey, and D. Quinlan (2004). The generalized earthquake-location  
572 (GENLOC) package: an earthquake-location library, *Computers & Geoscience*, **30(9-10)**, 1079-  
573 1091, <https://doi.org/10.1016/j.cageo.2004.06.010>.
- 574
- 575 Peck, W., B. W. Selleck, M. S. Wong, J. R. Chiarenzelli, K. S. Harpp, K. Hollocher, J. S.  
576 Lackey, J. Catalano, S. P. Regan, and A. Stocker (2013). Orogenic to postorogenic (1.20-1.15  
577 Ga) magmatism in the Adirondack Lowlands and Frontenac terrane, southern Grenville  
578 Province, USA and Canada, *Geosphere*, **9:6**, 1637-1663, doi:10.1130/GES00879.1.
- 579
- 580 Pierre, J-R, and M. Lamontagne (2004). The 20 April 2002, MW 5.0 Au Sable Forks, New York,  
581 earthquake; a supplementary source of knowledge on earthquake damage to lifelines and  
582 buildings in eastern North America, *Seism Res Lett*, **75**, 626–636.
- 583
- 584 Prigmore, J.K., A.J. Butler, N.H. Woodcock (1997). Rifting during separation of eastern  
585 Avalonia from Gondwana: evidence from subsidence analysis. *Geology* **25** 203–206
- 586
- 587 Regan, S.P., G.J. Walsh, M.L. Williams, J.R. Chiarenzelli, M. Toft, and R. McAleer, (2019),  
588 Syn-collisional exhumation of hot middle crust in the Adirondack Mountains (New York, USA):

- 589 Implications for extensional orogenesis in the southern Grenville province, *Geosphere*, **15(4)**, p.  
590 1240–1261, <https://doi.org/10.1130/GES02029.1>.
- 591
- 592 Revetta, F.A. (2004) Interpretation of Local Gravity Anomalies in Northern New York,  
593 *American Geophysical Union, Spring Meeting 2004*, abstract id. S21A-06
- 594
- 595 Rivers, T., and D. Corrigan, (2000). Convergent margin on southeastern Laurentia during the  
596 Mesoproterozoic: Tectonic implications, *Canadian Journal of Earth Sciences*, **37**, p. 359–383,  
597 doi: 10.1139/cjes-37-2-3-359.
- 598
- 599 Rivers, T., (2008). Assembly and preservation of lower, mid, and upper orogenic crust in the  
600 Grenville Province—Implications for the evolution of large, hot, long-duration orogens,  
601 *Precambrian Research*, **167**, p. 237–259, <https://doi.org/10.1016/j.precamres.2008.08.005>.
- 602
- 603 Roden-Tice, M.K., A. Tremblay, K.M. Negrycz, and B. Gamache (2012). Mesozoic unroofing of  
604 the Ottawa-Bonnechere Graben, Ontario, based on apatite fission-track thermochronology, In  
605 *Geological Society of America Abstracts with Programs*, **44:69**.
- 606
- 607 Seeber, L. and J. G. Armbruster (1986). A Study of Earthquake Hazard in New York State, and  
608 Adjacent Areas, report to the U.S. Nuclear Regulatory Commission, NUREG CR-4750, 98 pp.
- 609

- 610 Seeber, L., Kim, W.Y., Armbruster, J., Du, W.X., and Lerner-Lam, A. 2002. The 20 April 2002  
611 MW5.0 earthquake near Au Sable Forks, Adirondacks, New York: A first glance at a new  
612 sequence. *Seismological Research Letter*, 73: 480–489.
- 613
- 614 Spencer, C. J., P. A. Cawood, C. J. Hawkesworth, A. R Prave, N. M.W. Roberts, M. S.A.  
615 Horstwood, M.J. Whitehouse, EIMF, (2015) Generation and preservation of continental crust in  
616 the Grenville Orogeny, *Geoscience Frontiers*, 6, 357-372.
- 617 <http://dx.doi.org/10.1016/j.gsf.2014.12.001>
- 618
- 619 Stump, B. W., Hedlin, M. A. H., Pearson, D. C., and Hsu, V., (2002) Characterization of mining  
620 explosions at regional distances: Implications with the International Monitoring System, *Rev.  
621 Geophys.*, 40(4), 1011, doi:[10.1029/1998RG000048](https://doi.org/10.1029/1998RG000048), .
- 622
- 623 U.S. Geological Survey, Earthquake Hazards Program, 2017, Advanced National Seismic  
624 System (ANSS) Comprehensive Catalog of Earthquake Events and Products: Various,  
625 <https://doi.org/10.5066/F7MS3QZH>.
- 626
- 627 Vermont DEC, List of Mine, quarry and sand and gravel pit status in 2014. Retrieved from:  
628 <https://dec.vermont.gov/geological-survey/resources-energy/minres>
- 629
- 630 Viegas, G.M., L.G. Baise, and R.E. Abercrombie (2011). Regional Wave Propagation in New  
631 England and New York, *Bulletin of the Seismological Society of America*, 100(5A), 2196-2218  
632 10.1785/0120090223.

- 633
- 634 Wiener, R.W., McLelland, J.M., Isachsen, Y.W., and Hall, L.M., (1984), Stratigraphy and  
635 structural geology of the Adirondack Mountains, New York: Review and synthesis, in  
636 Bartholomew, M.J., ed., *The Grenville event in the Appalachians and related topics: Geological*  
637 *Society of America Special Paper* **194**, p. 1–55.
- 638
- 639 Yang, X., and H. Gao, (2018). Full-Wave Seismic Tomography in the Northeastern United  
640 States: New Insights Into the Uplift Mechanism of the Adirondack Mountains, *Geophysical*  
641 *Research Letters*, **45**, 5992-6000. <https://doi.org/10.1029/2018GL078438>
- 642
- 643 Yaun, H., S. French, P. Cupillard, and B. Romanowicz, (2014). Lithospheric expression of  
644 geological units in central and eastern North America from full waveform tomography, *Earth*  
645 *and Planetary Science Letters*, **402**, 176-186. <http://dx.doi.org/10.1016/j.epsl.2013.11.057>
- 646
- 647 Zartman, R. E. (1977). Geochronology of some alkalic rock provinces in eastern and central  
648 United States, *Annual Review of Earth and Planetary Sciences*, **5(1)**, 257–286.  
649 <https://doi.org/10.1146/annurev.ea.05.050177.001353>
- 650
- 651

652 Mailing Addresses of Authors:

653

654 Adams, Jin, and Dimas:

655 Colgate University

656 Department of Geology

657 13 Oak Dr.

658 Hamilton, NY 13346

659

660 Dove:

661 University of Rhode Island

662 Narragansett Bay Campus

663 215 South Ferry Road

664 Narragansett, RI 02882

665

666 Figure Captions:

667

668 Figure 1. Major Geologic Features. The Taconic Suture separating the Grenville and

669 Appalachian Provinces is shown by a solid white line. The outline of the Adirondack Mountains

670 is marked by a dashed white line, and the exposure of the Marcy Massif within the Adirondack

671 Mountains is outlined in black. Earthquakes recorded in the past century are shown by white

672 dots, and earthquakes with magnitudes greater than 4.5 during the past century are shown by

673 black circles, scaled by magnitude (U.S Geological Survey). Political boundaries are shown in

674 black, with international boundaries shown as solid lines and state and province boundaries

675 shown as dashed lines. Details on earthquakes with  $M > 4.5$  are given in Table 1.

676 ADH=Adirondack Highlands; ADL=Adirondack Lowlands; WQSZ=Western Quebec Seismic

677 Zone; TS=Taconic Suture; MV=Mohawk Valley; NHV=North Hudson Valley.

678

679 Figure 2. Locations of stations used in the study. Stations outlined in white are assigned to the

680 Appalachian velocity model (Viegas et al., 2010) during relocations with Hypoinverse. Symbols

681 denoting important geologic boundaries are the same as in Figure 1.

682

683 Figure 3. Regional velocity models used for relocations (Viegas et al., 2010), compared to global

684 average velocity models IASP91 and PREM.

685

686 Figure 4. Sample of vertical seismograms displaying characteristics of (a) a regional earthquake

687 and (b) a typical mining event. Seismograms are ordered by distance from the origin, with the

688 origin time set to zero, and bandpass filtered between 1-10 Hz.

689

690 Figure 5. Locations of mining events (a) and earthquakes (b) following preliminary location in  
691 Antelope. Symbols denoting important geologic boundaries are the same as in Figure 1.

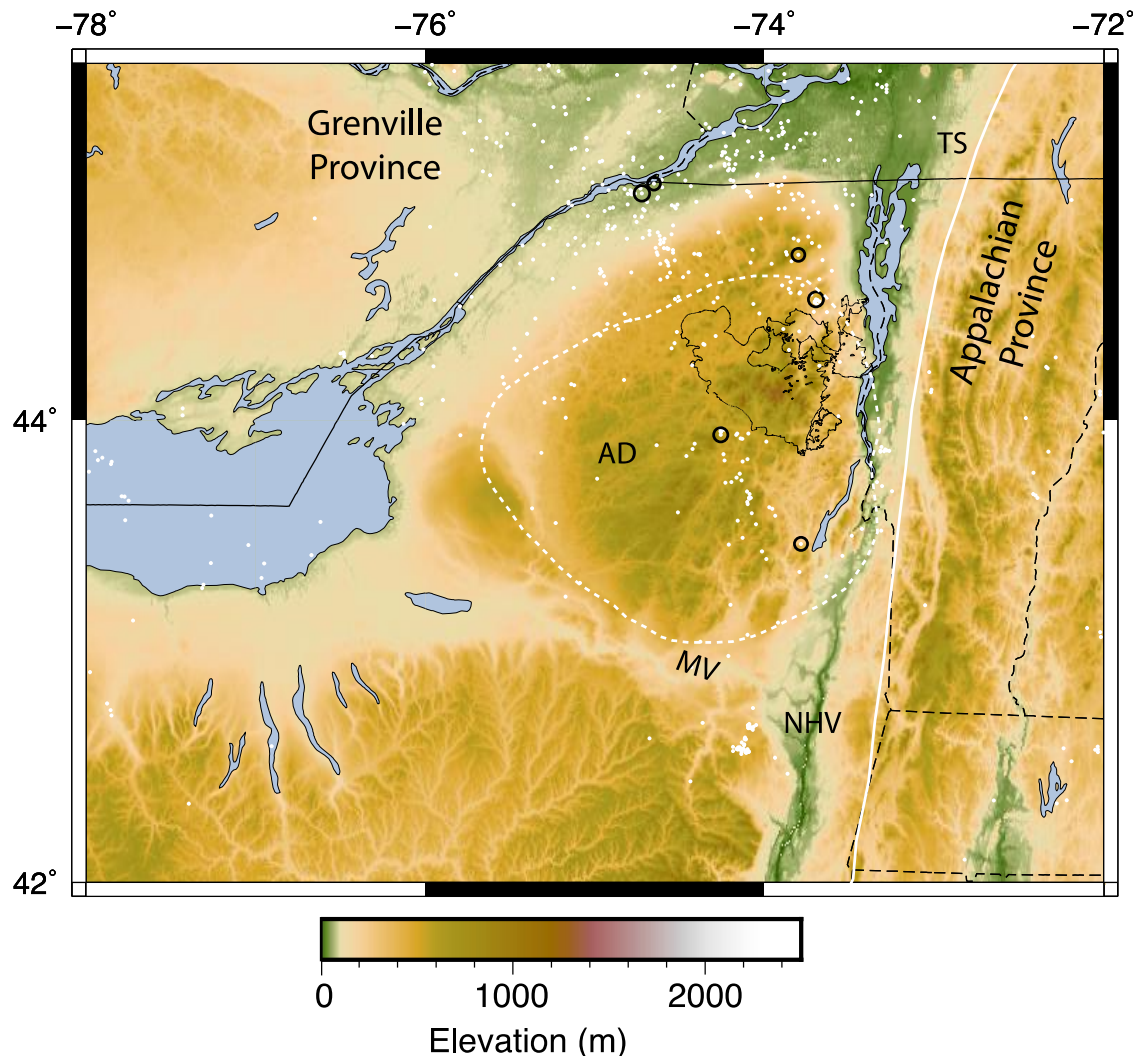
692

693 Figure 6. Locations of mining events (a) and earthquakes (b) following relocation using two  
694 regional velocity models in Hypoinverse. Symbols denoting important geologic boundaries are  
695 the same as in Figure 1.

696

697

698 Figures:

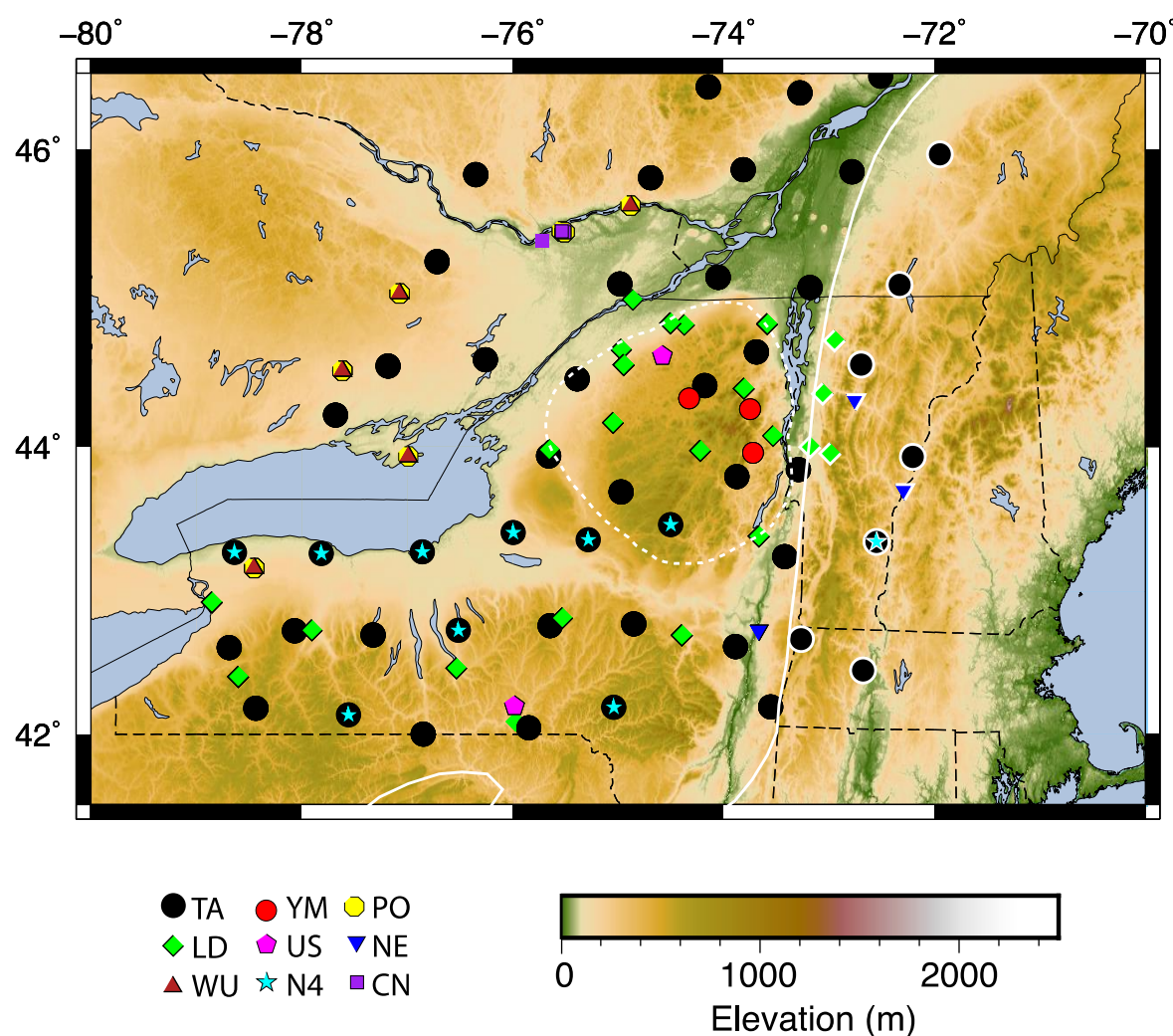


699

700 Figure 1. Major Geologic Features. The Taconic Suture separating the Grenville and  
701 Appalachian Provinces is shown by a solid white line. The outline of the Adirondack Mountains  
702 is marked by a dashed white line, and the exposure of the Marcy Massif within the Adirondack  
703 Mountains is outlined in black. Earthquakes recorded in the past century are shown by white  
704 dots, and earthquakes with magnitudes greater than 4.5 during the past century are shown by  
705 black circles, scaled by magnitude (U.S Geological Survey). Political boundaries are shown in  
706 black, with international boundaries shown as solid lines and state and province boundaries

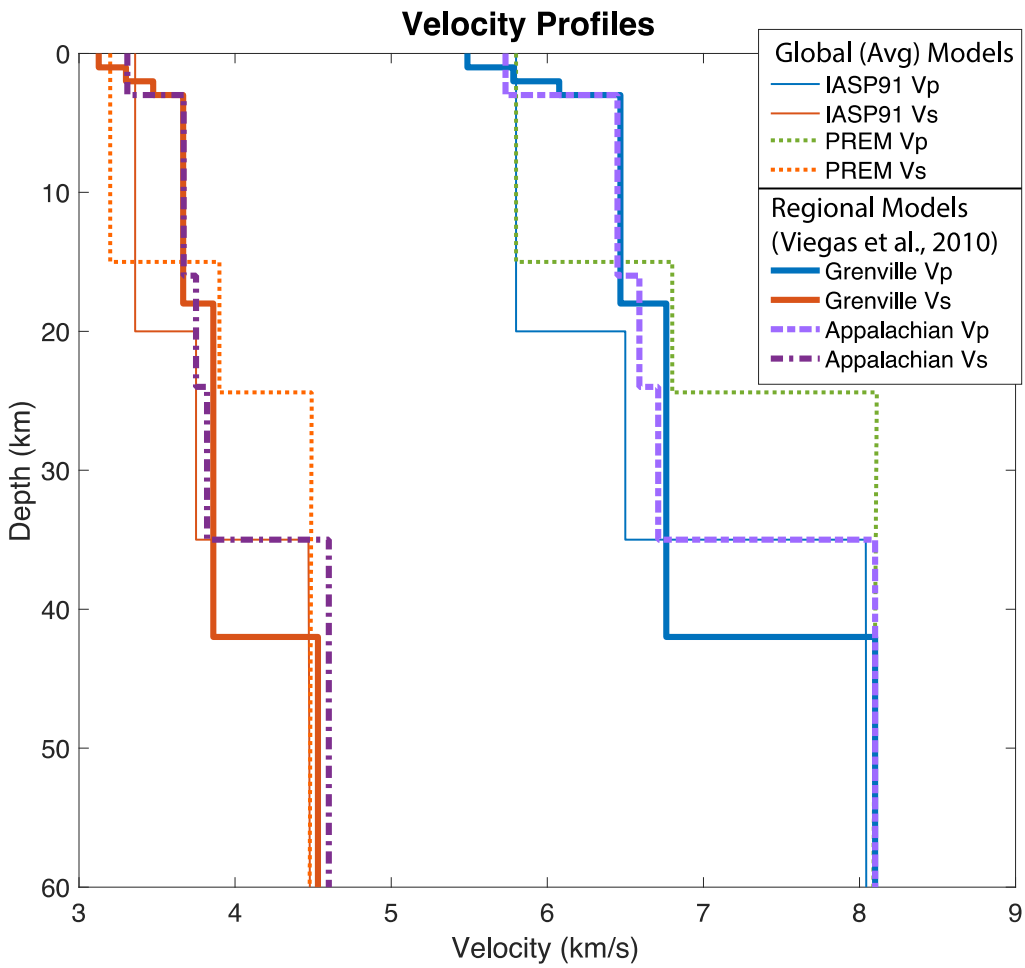
707 shown as dashed lines. Details on earthquakes with  $M > 4.5$  are given in Table 1.  
708 ADH=Adirondack Highlands; ADL=Adirondack Lowlands; WQSZ=Western Quebec Seismic  
709 Zone; TS=Taconic Suture; MV=Mohawk Valley; NHV=North Hudson Valley.

710



711  
712 Figure 2. Locations of stations used in the study. Stations outlined in white are assigned to the  
713 Appalachian velocity model (Viegas et al., 2010) during relocations with Hypoinverse. Symbols  
714 denoting important geologic boundaries are the same as in Figure 1.

715

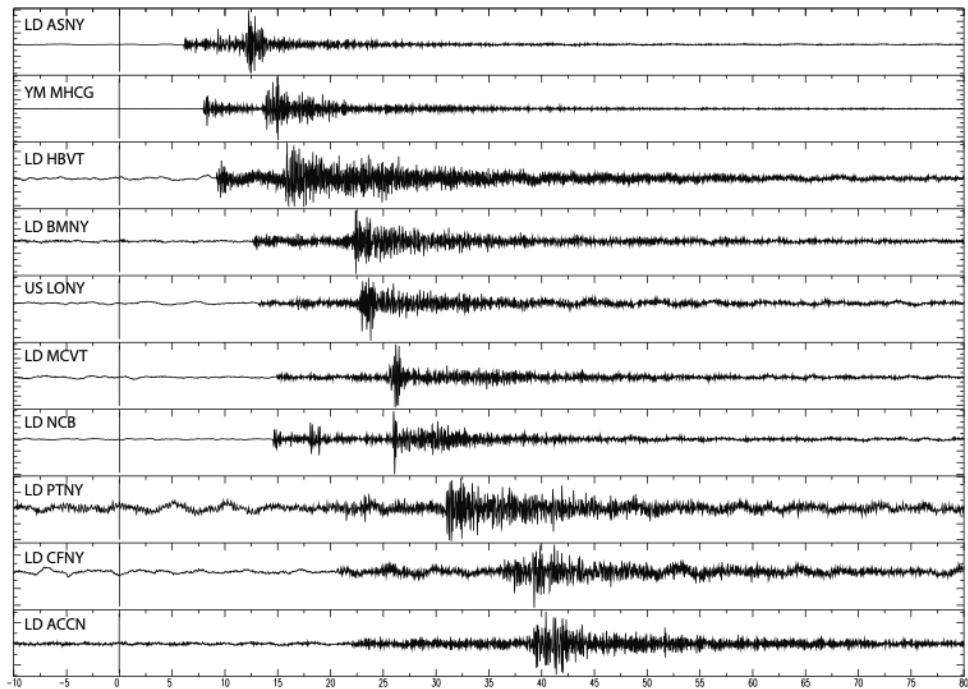


716

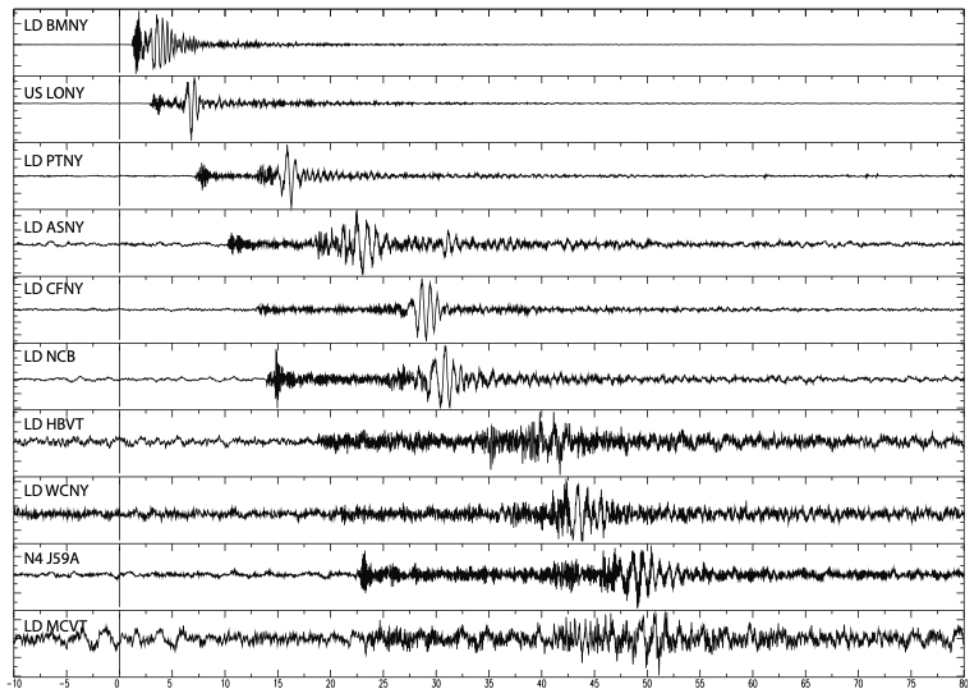
717 Figure 3. Regional velocity models used for relocations (Viegas et al., 2010), compared to global  
718 average velocity models IASP91 and PREM.

719

a) Earthquake 01/21/2017 15:35



b) Mine Event 07/05/2016 17:23



720

721 Figure 4. Sample of vertical seismograms displaying characteristics of (a) a regional earthquake  
722 and (b) a typical mining event. Seismograms are ordered by distance from the origin, with the  
723 origin time set to zero, and bandpass filtered between 1-10 Hz.

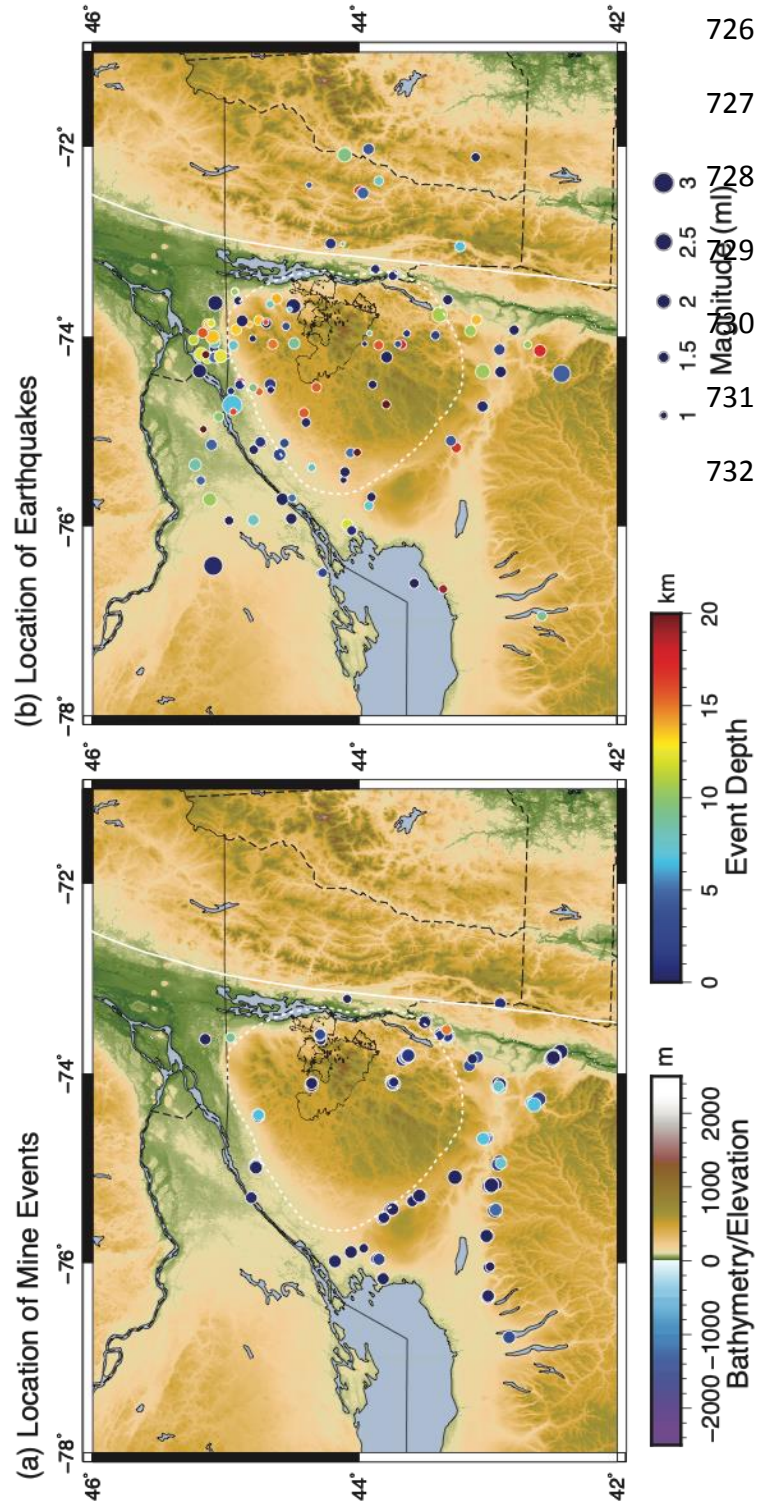
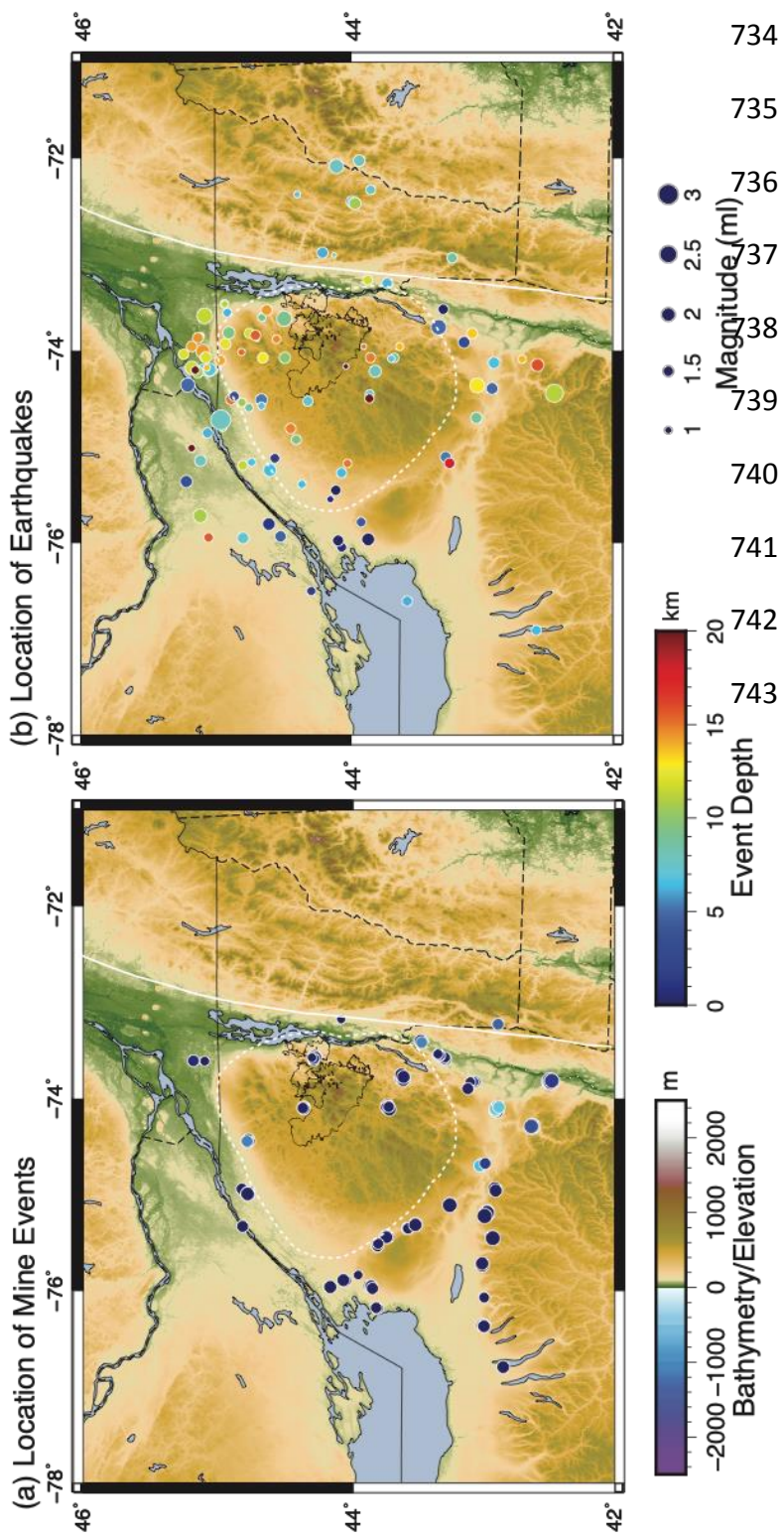


Figure 5. Locations of mining events (a) and earthquakes (b) following preliminary location in Antelope. Symbols denoting important geologic boundaries are the same as in Figure 1.

733



734 Figure 6. Locations of mining  
735 events (a) and earthquakes (b)  
736 following relocation using  
737 two regional velocity models  
738 in Hypoinverse. Symbols  
739 denoting important geologic  
740 boundaries are the same as in  
741 Figure 1.

744 Tables:

745

746 Table 1. Moderate-Sized Earthquakes (Preferred Mag $\geq$  4.5) 1917-2017 from ANSS Catalog

Magnitude	Date	Time (UTC)	Latitude	Longitude	Depth	Location
5.3 M <sub>Lg</sub>	04/20/2002	10:50:47	44.51	-73.70	4.8	Au Sable Forks, NY
5.1 M <sub>b</sub>	10/07/1983	10:18:46	43.94	-74.26	12.5	Newcombe, NY (Goodnow)
4.5 M <sub>Lg</sub>	09/05/1944	08:51:06	45.00	-74.65	1.0	NY-Ontario Border
5.5 M <sub>w</sub>	09/05/1944	04:38:45	44.96	-74.72	12.0	NY-Ontario Border (Massena)
4.5 M <sub>I</sub>	04/15/1934	02:58:13	44.70	-73.80	-	Johnson Mountain, NY
4.7 M <sub>Lg</sub>	04/20/1931	19:54:30	43.47	-73.78	5.0	Warrensburg, NY

747

Figure 1

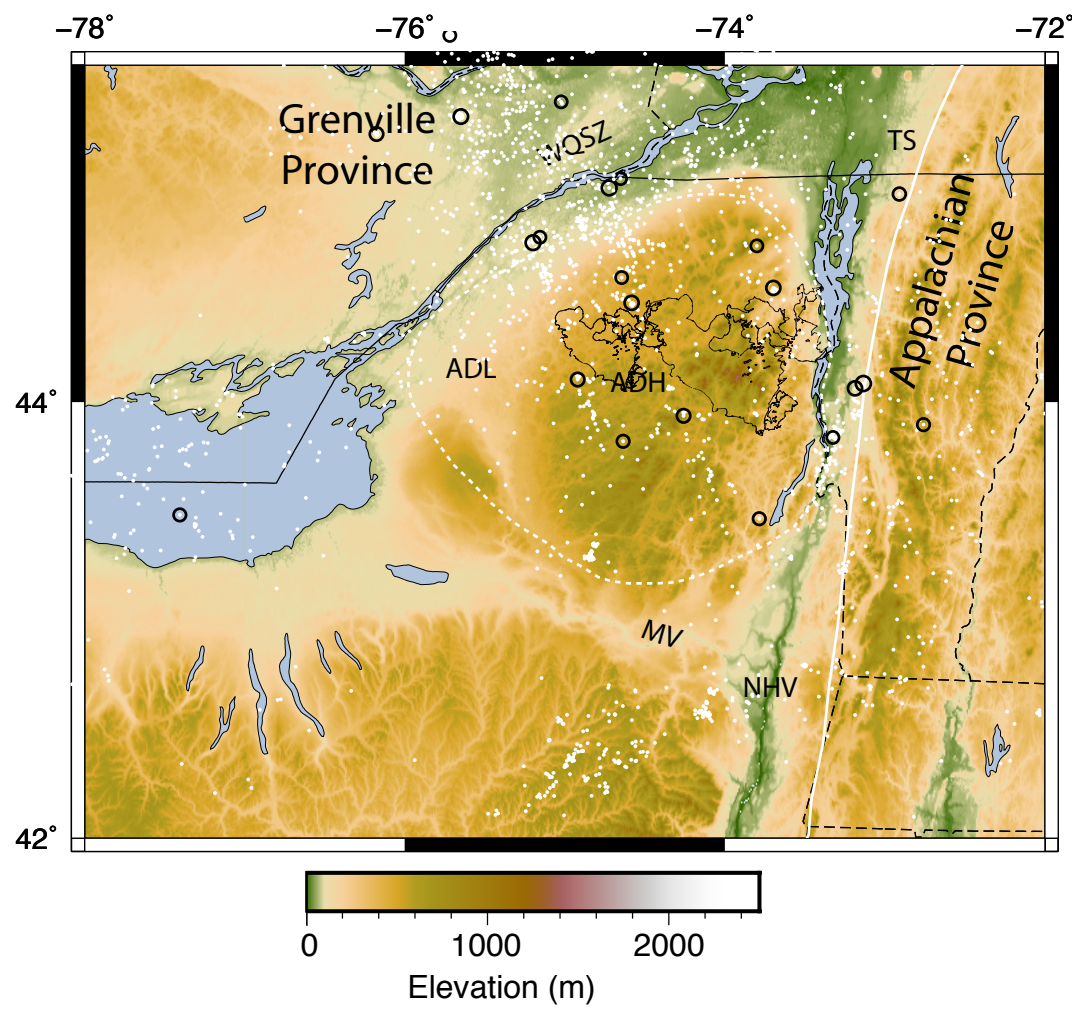
[Click here to access/download;Figure;Figure1adirmap.pdf](#)

Figure 2

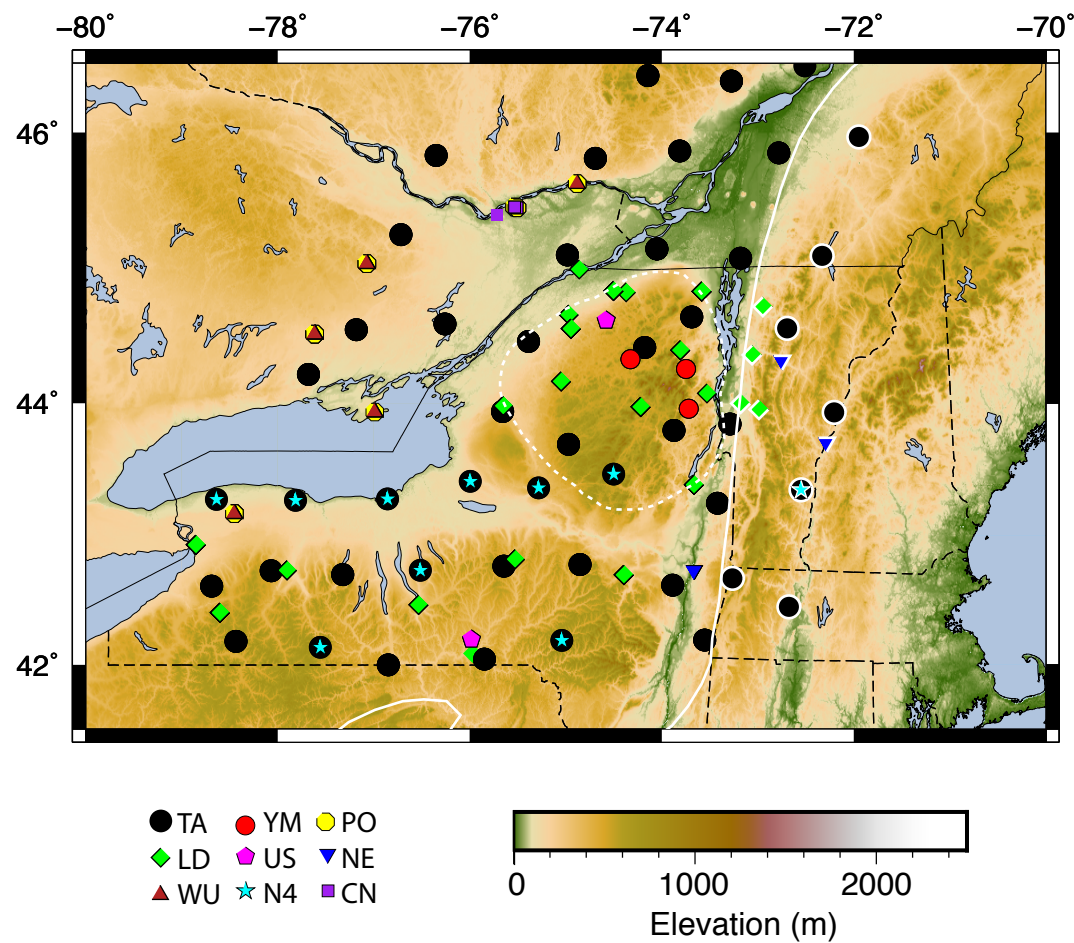
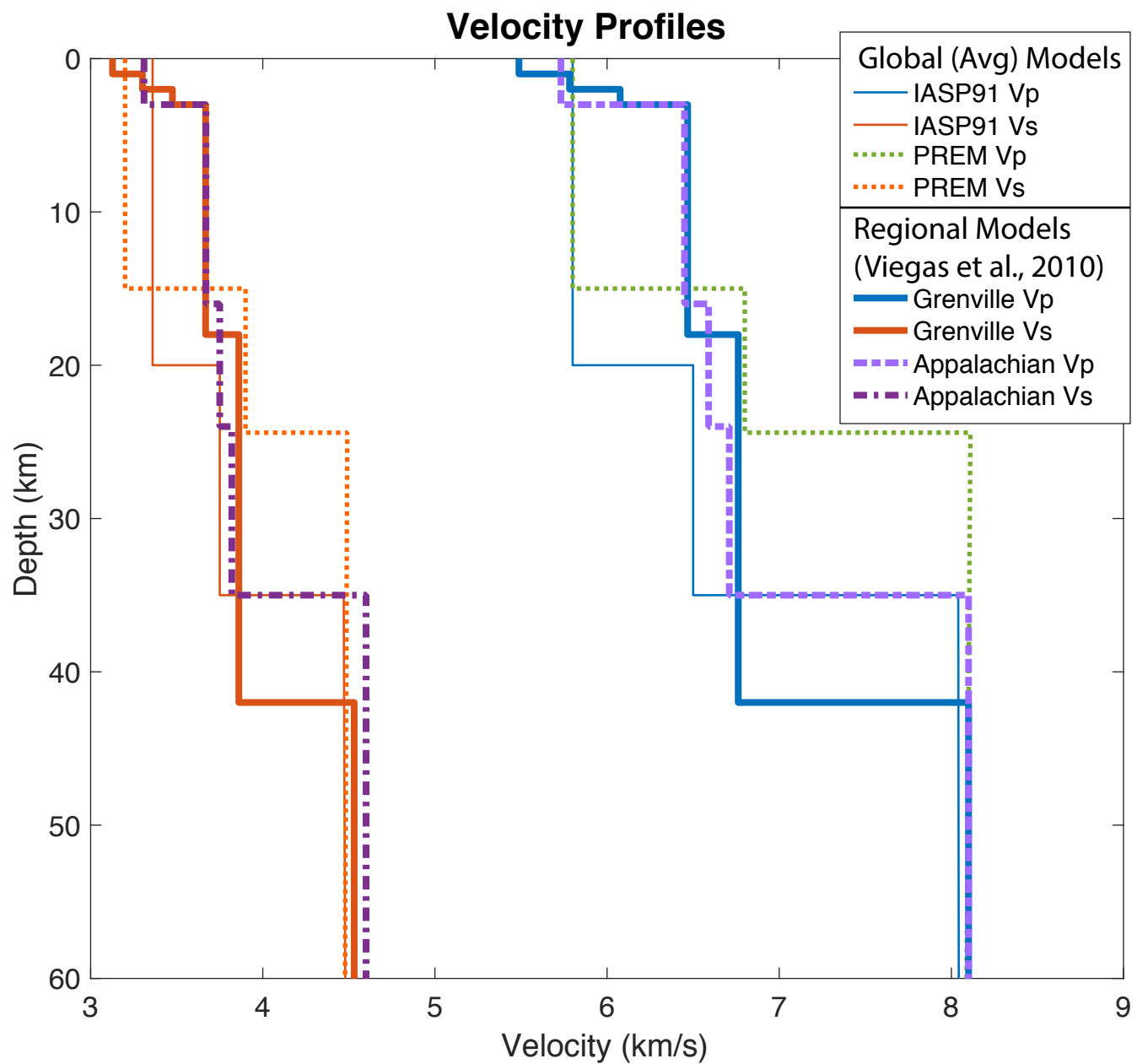
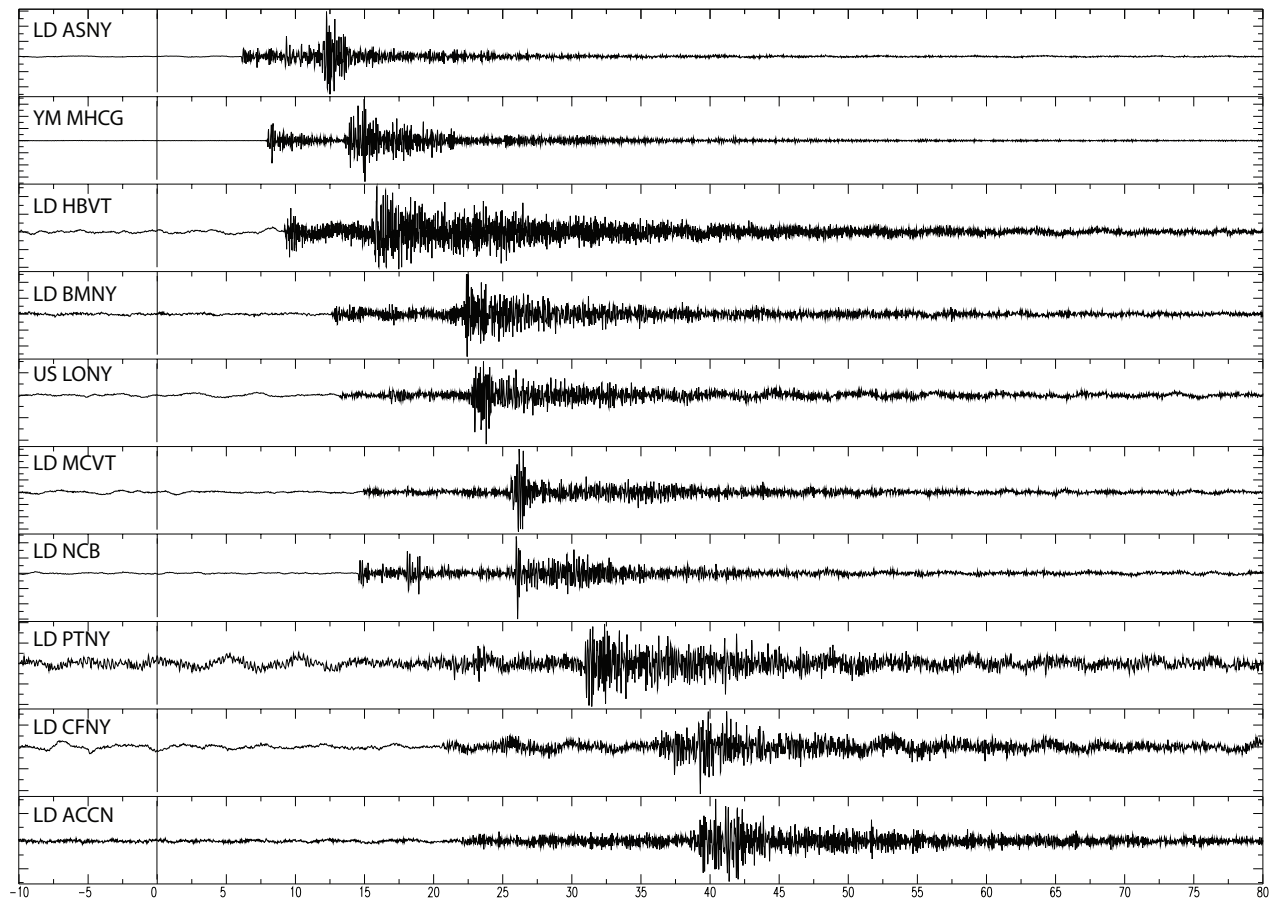
[Click here to access/download;Figure;Figure2adirstamap.pdf](#)

Figure 3

Click here to  
access/download;Figure;Figure3\_AdirondackVelocities.pdf



a) Earthquake 01/21/2017 15:35



b) Mine Event 07/05/2016 17:23

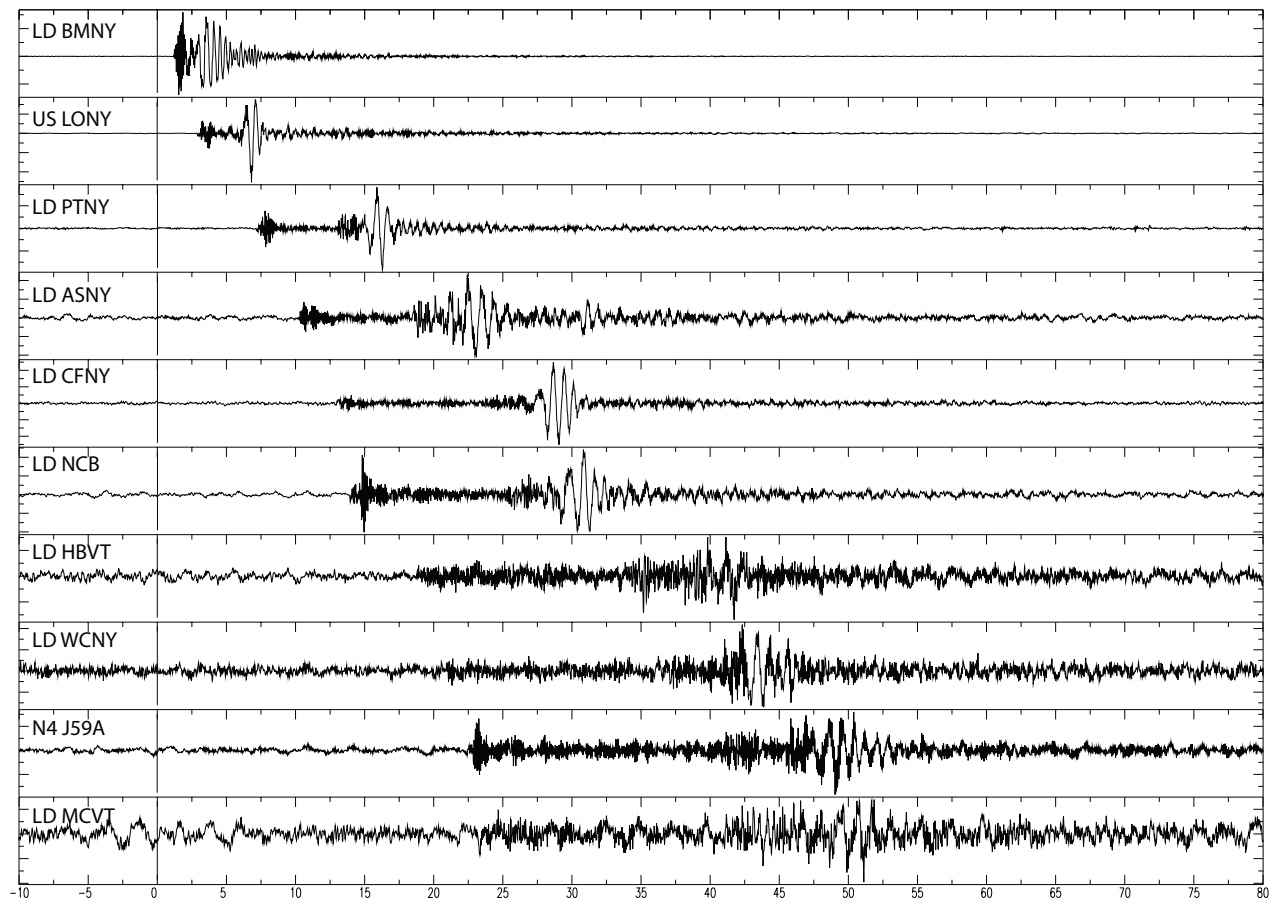
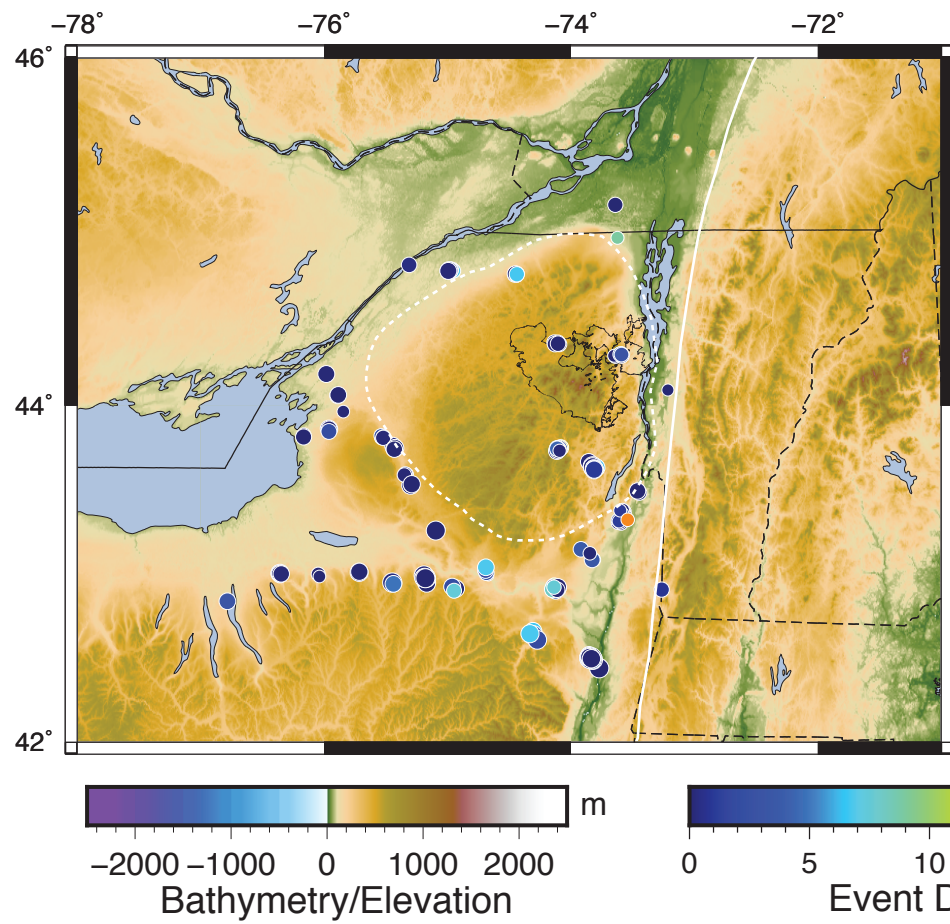


Figure 5

[Click here to access/download;Figure;Figure5\\_AntelopeLocations.pdf](#)

(a) Location of Mine Events



(b) Location of Earthquakes

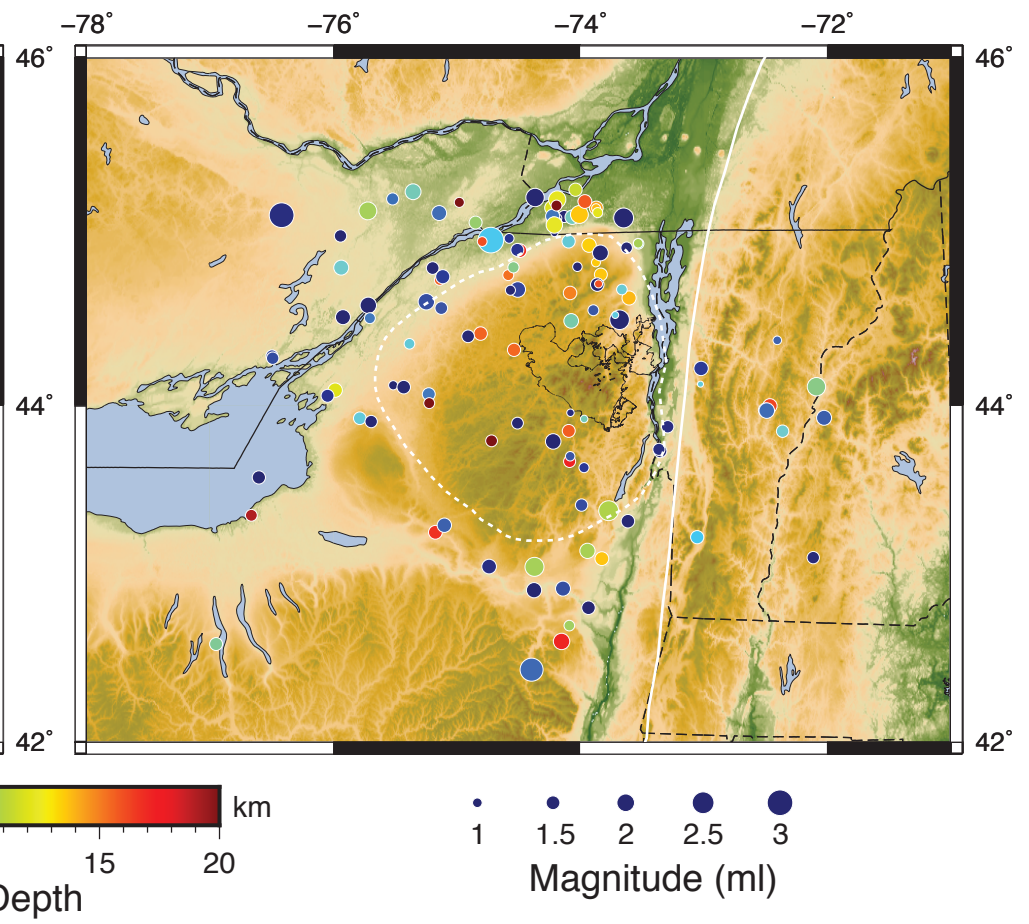
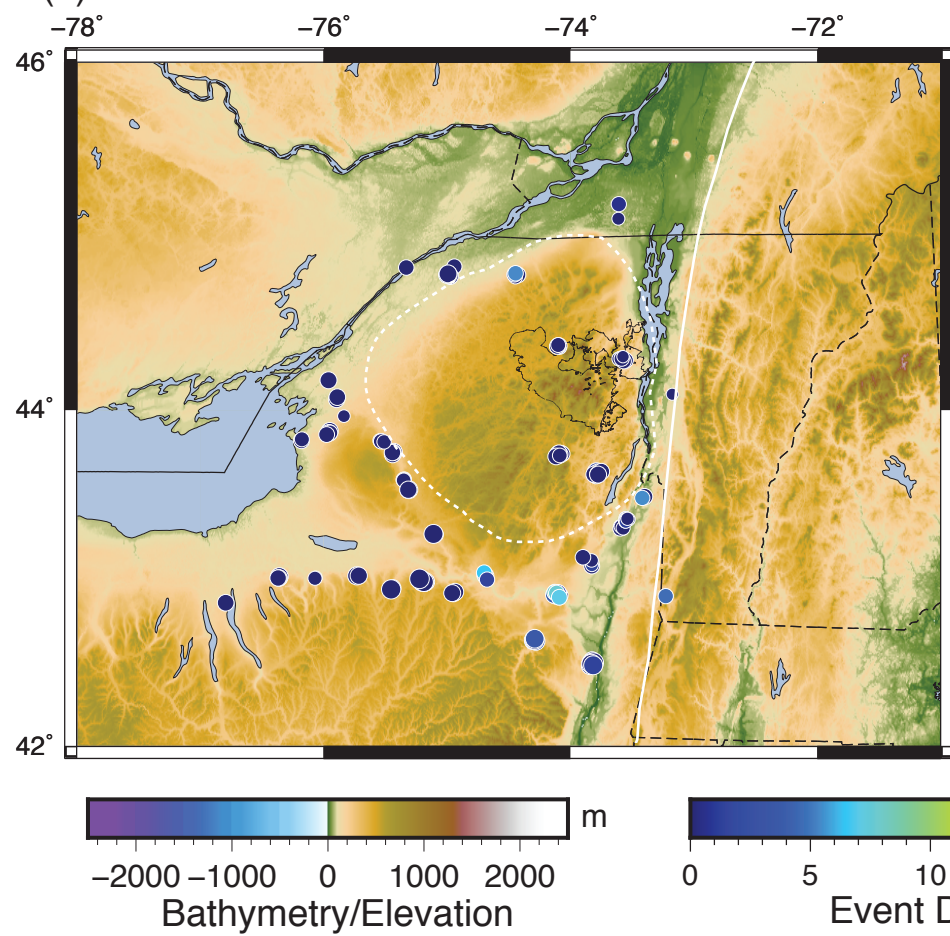


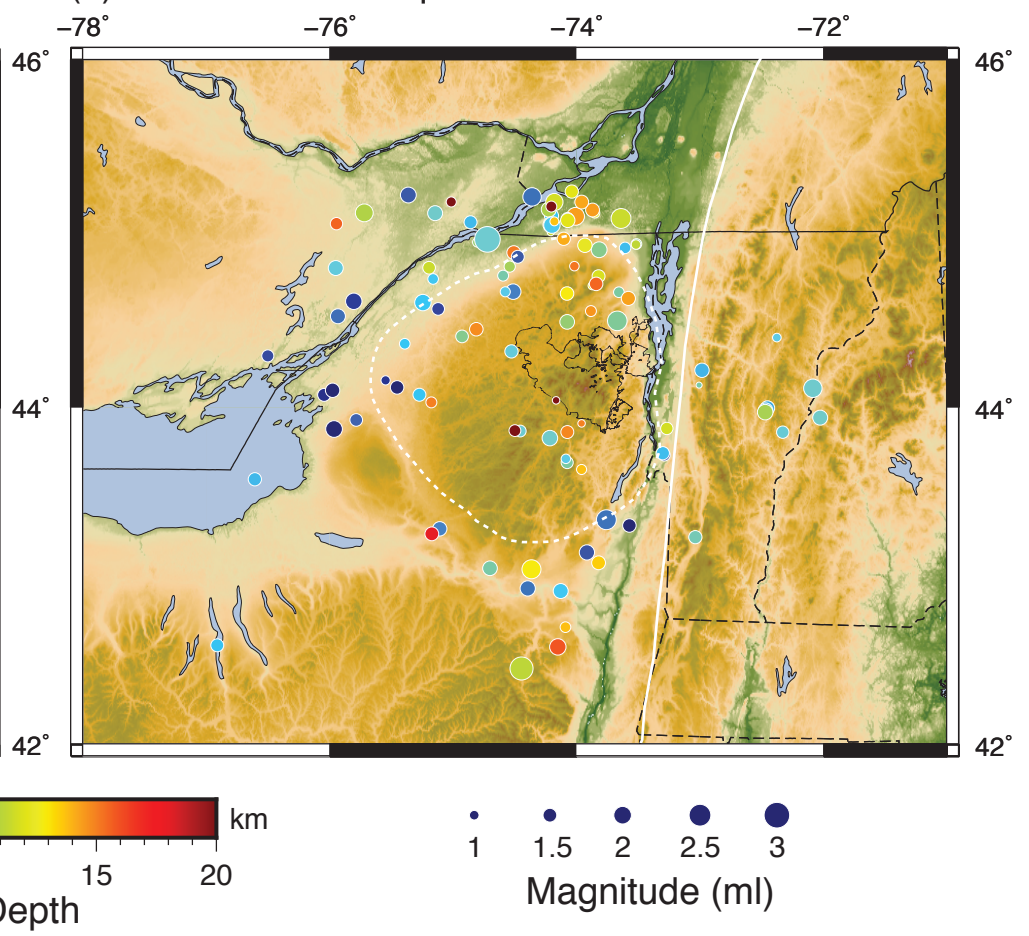
Figure 6

[Click here to access/download;Figure;Figure6\\_HypolnverseLocations.pdf](#)

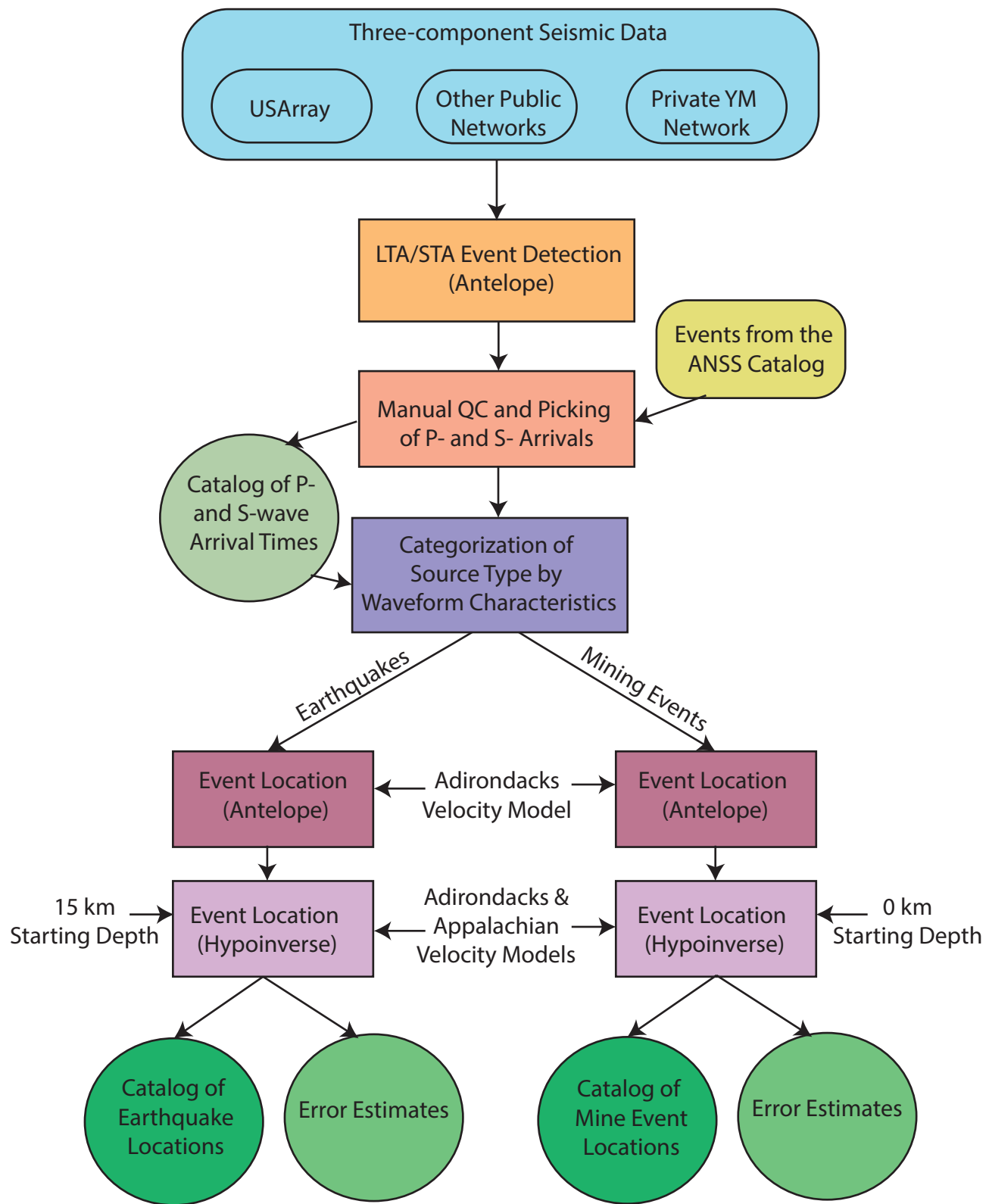
(a) Location of Mine Events



(b) Location of Earthquakes



## Appendix Figure A1 - Methodology Flow Chart



Appendix Table A2 - Mine Event Locations and Errors

	Notes	ORID	Type	Time and Date						Location			Horz Error km	Vert Error km	RMS Err	Max Azimuth	Closest Station (km)	Number of Arrivals			Magnitude (ml)	# Mag Stations
				Year	Month	Day	Hour	Minute	Second	Latitude	Longitude	Depth km						P	S	Total		
	115757	MN	2013	4	5	20	35	46.18	43.7457	-74.0748	0.00	0.4	1.3	0.19	66	28.0	8	8	10	2.04	16	
	115759	MN	2013	4	26	17	44	25.60	44.3672	-74.0875	0.76	0.2	0.9	0.10	112	45.1	9	7	10	1.78	16	
X	115763	MN	2013	5	28	19	56	55.38	43.7432	-74.0672	0.00	1.1	4.4	0.45	137	28.5	9	7	11	1.98	16	
Z	115696	MN	2013	9	16	16	31	21.06	44.7272	-74.4125	0.00	1.4	7.3	0.44	84	18.0	9	3	11	1.71	12	
	3384	MN	2013	9	19	15	57	16.77	43.8777	-75.9487	0.00	0.3	1.3	0.32	46	24.1	21	26	32	2.13	47	
	115769	MN	2013	9	19	18	8	32.75	44.8283	-75.3290	0.00	0.6	1.4	0.22	129	40.9	5	6	7	1.95	11	
	3536	MN	2013	9	21	13	10	43.39	42.9132	-74.9452	0.00	0.5	1.6	0.24	102	17.1	9	9	14	1.88	18	
	3392	MN	2013	9	24	14	33	33.60	43.7450	-75.4338	0.00	0.5	1.6	0.34	44	28.1	16	19	25	1.86	35	
	3289	MN	2013	9	30	15	54	42.04	42.6425	-74.3077	5.75	0.5	0.8	0.26	103	9.6	24	14	31	2.04	38	
	3429	MN	2013	10	1	15	58	43.69	43.5958	-75.3443	4.17	0.4	2.2	0.37	53	26.6	22	26	39	1.72	48	
	3291	MN	2013	10	4	15	18	53.88	42.9913	-75.1992	0.00	0.6	1.8	0.49	41	37.2	26	29	43	2.41	55	
	3468	MN	2013	10	14	18	1	2.85	43.3578	-73.5295	0.00	0.6	1.6	0.31	87	11.6	16	12	23	1.67	28	
	115724	MN	2013	10	17	19	33	37.00	43.3073	-73.5895	0.01	0.5	1.0	0.19	96	10.7	13	9	18	1.69	22	
	3470	MN	2013	10	21	18	52	47.87	42.5027	-73.8202	0.00	0.4	1.1	0.28	105	13.9	26	21	34	2.09	47	
	3371	MN	2013	10	29	21	20	20.70	42.5042	-73.8088	0.00	0.6	1.6	0.42	104	40.4	26	21	36	2.27	47	
	3349	MN	2013	11	4	20	15	45.31	43.7423	-74.0952	0.00	0.3	1.0	0.28	54	18.8	24	28	36	2.11	52	
	115748	MN	2013	11	11	17	4	6.45	43.3637	-73.5503	0.00	0.5	1.4	0.19	107	9.8	17	5	20	1.72	22	
	3293	MN	2013	11	12	16	20	57.10	43.0122	-76.3590	0.00	0.3	1.0	0.27	39	33.7	33	21	37	2.01	54	
	115750	MN	2013	12	4	15	53	52.27	43.3023	-73.5792	0.00	0.4	1.0	0.26	66	11.6	15	15	23	1.72	30	
	115771	MN	2013	12	12	19	43	50.22	44.2990	-73.6068	0.00	0.7	2.5	0.35	108	39.1	10	7	14	1.73	17	
	115773	MN	2013	12	19	18	30	58.94	43.0812	-73.8272	0.00	0.6	1.6	0.28	167	36.1	15	10	20	1.98	25	
	3450	MN	2013	12	20	21	54	1.46	42.4998	-73.8310	0.00	0.5	1.5	0.31	106	13.8	19	16	27	2.31	35	
	3298	MN	2014	1	10	17	47	1.39	43.0180	-76.3670	0.00	0.4	1.2	0.32	40	34.1	26	23	35	1.92	49	
	3475	MN	2014	1	14	18	26	13.83	42.5077	-73.8343	0.00	0.5	1.3	0.38	105	12.9	22	30	37	2.16	52	
	3325	MN	2014	2	12	21	22	40.94	42.4967	-73.8257	0.00	0.7	1.9	0.47	106	40.4	24	19	33	2.36	43	
	3259	MN	2014	2	19	18	2	39.07	43.0153	-76.3597	0.00	0.4	1.2	0.36	39	34.0	30	22	39	2.18	52	
	3313	MN	2014	3	5	17	55	16.15	42.9157	-74.1203	0.00	0.4	1.3	0.32	74	33.3	32	19	38	1.77	51	
	3303	MN	2014	3	10	17	29	22.38	43.7418	-74.0820	0.00	0.4	1.1	0.32	54	17.8	28	21	36	1.96	49	
	3452	MN	2014	3	18	20	2	28.34	42.4937	-73.8333	0.00	0.6	1.4	0.41	107	14.4	30	24	39	2.11	54	
	3319	MN	2014	3	25	16	2	22.13	42.9120	-74.1167	4.26	0.3	1.0	0.22	74	33.2	26	13	31	1.89	39	
	3454	MN	2014	3	27	16	19	28.09	42.6325	-74.2788	2.07	0.5	1.0	0.29	135	12.1	32	24	40	2.28	56	
	3309	MN	2014	4	9	17	40	6.46	44.3808	-74.0955	0.00	0.4	1.2	0.35	39	7.9	27	23	31	1.76	50	
	3342	MN	2014	4	15	16	31	3.39	43.6335	-73.7863	0.00	0.4	1.2	0.21	85	19.4	16	13	21	2.17	29	
	115746	MN	2014	4	17	14	10	11.75	43.3175	-73.5978	0.37	0.7	1.5	0.20	121	9.3	10	5	10	1.58	15	
	3373	MN	2014	4	23	18	48	46.02	44.3045	-73.5872	0.00	0.5	2.1	0.25	47	38.8	19	7	21	1.72	26	
	115722	MN	2014	4	24	16	38	37.33	43.3015	-73.5967	0.00	0.7	1.7	0.34	81	10.9	13	11	18	1.79	24	
	3307	MN	2014	4	24	16	53	27.71	43.7547	-75.4305	0.00	0.6	2.4	0.45	72	27.4	14	14	20	2.19	28	
	3434	MN	2014	4	29	14	56	17.05	43.5922	-75.3510	0.00	0.3	0.9	0.31	38	26.3	25	30	41	1.85	55	
	3328	MN	2014	5	1	14	55	47.18	43.0238	-74.6882	0.00	0.4	1.3	0.23	64	30.7	32	10	36	2.10	42	
	3446	MN	2014	5	1	18	45	51.29	44.2942	-73.5598	0.00	0.5	1.9	0.30	92	40.3	14	11	16	1.81	25	
	3304	MN	2014	5	2	15	45	13.84	43.0172	-76.3600	0.00	0.4	1.5	0.31	33	34.2	27	17	34	2.00	44	
	115730	MN	2014	5	6	17	15	35.56	44.3780	-74.1007	0.00	0.7	2.0	0.33	117	44.1	9	9	14	1.83	18	
	3285	MN	2014	5	7	16	13	35.50	42.6393	-74.2922	1.66	0.5	1.4	0.25	134	10.8	26	12	30	2.24	38	
	3459	MN	2014	5	8	14	39	59.60	42.9100	-74.0972	4.31	0.3	1.2	0.23	75	34.2	19	15	25	1.85	34	
	3477	MN	2014	5	9	15	54	51.45	43.5905	-75.3528	0.00	0.4	1.4	0.35	52	26.2	21	27	35	1.78	48	
	3281	MN	2014	5	14	16	41	23.78	42.9897	-75.1845	0.00	0.5	1.7	0.52	41	36.1	26	30	43	2.31	56	
	3277	MN	2014	5	14	18	0	3.38	43.6340	-73.7800	0.00	0.4	1.7	0.35	71	19.5	26	18	32	2.13	44	
	115761	MN	2014	5	16	16	0	39.45	43.3652	-73.5525	0.23	0.5	1.1	0.18	98	9.6	13	5	15	1.60	18	
	3354	MN	2014	5	20	16	2	4.76	44.3760	-74.0887	0.00	0.5	1.1	0.30	69	8.6	15	16	20	1.87	31	
	115691	MN	2014	5	20	20	49	25.60	42.5227	-73.8245	0.00	0.6	1.8	0.32	103	42.8	26	12	31	1.97	38	
	3341	MN	2014	5	23	18	2	32.52	43.5263	-75.3072	0.00	0.4	1.4	0.26	60	18.5	14	12	21	1.63	26	
	115783	MN	2014	5	27	16	26	24.09	43.0112	-74.6835	0.00	1.4	4.2	0.28	183	29.7	6	6	10	1.33	12	

		115732	MN	2014	5	30	15	53	26.27	43.3150	-73.5915	0.00	0.4	1.0	0.13	85	9.9	13	4	14	1.67	17
		115728	MN	2014	5	30	16	24	54.75	44.8335	-74.9403	0.00	2.0	4.6	0.61	131	30.2	8	7	11	1.89	15
		3461	MN	2014	6	2	15	40	14.73	42.9295	-74.1267	0.51	0.4	1.4	0.24	91	61.8	13	17	23	1.80	30
		3283	MN	2014	6	5	15	33	3.12	43.0197	-76.3577	0.00	0.4	1.2	0.37	33	34.6	24	27	40	2.24	51
		3305	MN	2014	6	9	15	16	8.03	42.9868	-75.1735	0.00	0.6	1.7	0.41	60	35.2	15	16	27	2.30	31
		3416	MN	2014	6	9	16	58	21.29	44.7770	-74.9753	0.00	0.5	1.4	0.31	95	35.7	21	16	28	1.79	37
		3338	MN	2014	6	16	16	15	27.97	44.7828	-74.9792	0.00	0.4	1.4	0.31	97	35.6	20	20	30	1.98	40
X	Z	115765	MN	2014	6	23	16	38	45.83	44.2782	-73.6112	0.00	2.0	5.8	0.74	125	41.3	8	7	10	1.59	15
		3316	MN	2014	6	24	16	28	49.87	44.7853	-74.4268	0.00	0.7	2.0	0.41	55	8.7	23	11	26	2.02	34
		3386	MN	2014	6	24	18	36	35.79	42.5065	-73.8268	0.00	0.6	1.5	0.37	105	13.3	19	18	26	2.33	37
		3351	MN	2014	6	25	17	21	49.79	43.0172	-76.3588	0.00	0.4	1.5	0.33	65	34.3	13	23	27	1.71	36
		3340	MN	2014	6	26	16	24	16.84	44.0627	-75.8938	0.00	0.4	1.3	0.27	60	21.2	19	19	27	2.07	38
		115726	MN	2014	6	27	17	25	10.83	43.1008	-73.8222	0.00	0.8	2.4	0.15	163	33.9	13	8	19	1.64	21
		115737	MN	2014	7	1	15	59	41.02	43.2688	-75.1085	0.00	0.5	1.4	0.30	54	17.6	16	16	28	1.78	32
		115739	MN	2014	7	2	16	59	54.62	43.0857	-73.8257	1.38	0.6	1.6	0.23	167	35.6	14	14	22	1.57	28
		3331	MN	2014	7	3	15	24	41.15	43.6348	-73.7850	0.00	0.4	1.6	0.29	71	19.3	20	15	26	2.19	35
		115752	MN	2014	7	8	15	31	36.97	43.3063	-73.5725	0.00	0.5	1.6	0.33	65	11.6	11	10	16	1.74	21
		3388	MN	2014	7	9	17	27	36.36	44.7770	-74.9742	0.00	0.5	1.6	0.42	78	35.6	33	22	38	2.07	55
		115776	MN	2014	7	10	16	0	58.69	45.1083	-73.6112	0.02	2.3	4.5	0.33	245	30.4	8	6	11	1.59	14
		3258	MN	2014	7	11	16	55	42.36	43.5328	-75.3087	0.00	0.4	1.4	0.37	55	19.3	28	25	39	2.27	53
		115755	MN	2014	7	16	15	59	36.29	43.3590	-73.5485	0.00	0.4	1.0	0.18	121	10.1	11	8	14	1.61	19
		3302	MN	2014	7	21	17	32	22.34	44.7830	-74.9815	0.00	0.6	2.0	0.40	41	35.6	21	15	26	1.98	36
		115693	MN	2014	7	24	15	31	52.60	43.8667	-75.9553	0.00	0.6	1.8	0.29	67	25.0	18	10	23	2.09	27
		3352	MN	2014	7	25	16	29	14.44	43.0083	-76.3570	0.00	0.3	0.8	0.22	65	33.4	25	30	35	1.97	55
		3278	MN	2014	7	25	18	30	18.96	43.6315	-73.7817	0.00	0.3	1.1	0.24	85	19.7	25	18	28	2.11	43
		3310	MN	2014	7	29	17	30	25.28	42.9823	-75.1820	0.00	0.7	2.1	0.53	42	35.4	20	20	32	2.28	40
		3297	MN	2014	7	30	14	27	43.22	43.0310	-74.6945	0.00	0.5	1.7	0.34	64	50.6	23	15	27	1.94	38
		3326	MN	2014	7	30	16	55	27.88	44.2900	-73.5537	0.00	0.5	1.9	0.39	48	40.0	23	18	28	1.98	41
		3419	MN	2014	7	30	17	17	19.99	42.6308	-74.3060	2.79	0.5	1.9	0.26	105	10.5	15	12	21	2.00	27
		3321	MN	2014	8	6	16	56	32.81	43.5925	-75.3512	0.00	0.4	1.2	0.28	46	26.3	25	22	36	1.72	47
		3528	MN	2014	8	18	14	3	7.27	42.9505	-75.4405	0.00	0.5	1.5	0.32	109	26.8	15	20	24	2.11	35
		3561	MN	2014	8	20	14	47	54.53	42.9013	-74.1153	6.55	0.4	0.8	0.20	113	32.4	16	13	23	1.98	29
		3276	MN	2014	8	21	16	45	4.54	43.6348	-73.7852	0.00	0.4	1.4	0.26	110	19.3	20	14	24	2.22	34
		3322	MN	2014	8	27	14	1	15.93	43.0415	-74.6985	6.50	0.5	0.9	0.25	63	49.6	28	12	34	1.96	40
		3400	MN	2014	8	28	15	56	19.42	43.5873	-75.3500	0.00	0.3	1.3	0.29	32	25.8	25	22	36	1.81	47
		3355	MN	2014	8	29	15	19	18.49	43.0227	-75.7305	0.00	0.5	2.1	0.40	64	29.6	17	14	23	2.30	31
		3403	MN	2014	8	29	19	21	4.05	42.4898	-73.8287	0.00	0.7	1.8	0.40	161	14.9	28	19	35	2.19	47
		3438	MN	2014	9	2	16	46	27.91	43.8672	-75.9473	0.00	0.4	1.4	0.33	61	24.4	21	22	31	1.95	43
		3532	MN	2014	9	3	16	59	57.06	43.1142	-73.8278	0.00	0.5	2.8	0.17	88	32.7	15	2	15	1.68	17
		3314	MN	2014	9	10	15	55	38.77	44.2852	-73.5677	0.00	0.5	1.7	0.37	66	41.2	24	15	28	1.92	39
		3534	MN	2014	9	12	15	49	39.90	42.8628	-76.7923	0.00	0.5	1.8	0.34	72	26.9	15	13	21	2.09	28
		3356	MN	2014	9	12	16	18	15.03	42.6343	-74.3012	4.54	0.4	1.0	0.27	104	10.6	25	16	34	1.93	41
		3360	MN	2014	9	15	14	11	46.72	43.9648	-75.8352	0.00	0.3	1.1	0.20	93	14.4	14	14	21	1.55	28
		3317	MN	2014	9	16	16	11	7.26	42.5078	-73.8280	0.00	0.8	1.8	0.48	104	13.1	30	17	34	2.09	47
		3481	MN	2014	9	16	16	41	14.54	44.3720	-74.1027	0.00	0.5	1.3	0.35	72	8.0	16	18	24	1.96	34
		3345	MN	2014	9	17	14	0	31.46	43.0007	-74.6750	1.50	0.5	1.5	0.32	70	29.0	21	13	25	1.90	34
		3405	MN	2014	9	18	14	55	7.17	42.9420	-75.4520	0.00	0.5	1.6	0.34	109	25.5	15	17	23	2.47	32
		3421	MN	2014	9	23	14	50	10.53	44.1743	-75.9595	0.00	0.6	1.8	0.44	53	32.5	23	23	34	2.15	46
		3282	MN	2014	9	24	16	38	9.88	43.0108	-76.3637	0.00	0.3	1.0	0.24	41	33.5	27	24	35	2.07	51
		3308	MN	2014	9	26	14	55	44.99	43.7390	-75.4398	0.00	0.7	2.1	0.41	87	28.3	18	13	21	2.07	31
		115717	MN	2014	9	26	15	20	43.06	43.0233	-75.7145	0.00	0.4	1.4	0.23	58	29.4	11	15	22	2.19	26
		3357	MN	2014	9	30	14	31	6.95	42.9090	-74.1337	3.81	0.4	2.3	0.23	111	32.0	23	9	24	2.10	32
		3407	MN	2014	10	14	14	34	57.62	42.9073	-74.0810	0.00	0.4	1.7	0.35	75	34.9	25	18	32	1.96	43
		3376	MN	2014	10	14	17	1	21.26	43.0103	-76.3682	0.00	0.4	1.3	0.35	40	33.3	26	18	35	2.07	44

		3514	MN	2014	10	14	19	13	11.87	44.0923	-73.1745	0.00	0.6	2.2	0.32	72	21.3	16	7	18	1.45	23
		115703	MN	2014	10	15	19	38	45.90	43.7410	-74.0948	0.00	0.5	1.8	0.25	93	18.8	12	10	15	1.98	22
		3485	MN	2014	10	21	19	57	36.68	44.7915	-74.9897	0.00	0.4	1.4	0.28	138	34.7	16	16	22	2.16	32
		3362	MN	2014	11	26	18	12	38.84	43.7508	-75.4335	0.00	0.5	1.9	0.35	85	27.6	17	13	22	1.95	30
		3423	MN	2014	12	1	20	1	43.93	42.4852	-73.8397	0.00	0.5	1.2	0.38	110	15.2	34	24	40	2.24	58
		3369	MN	2014	12	17	21	26	53.15	42.5008	-73.8222	0.00	0.6	2.3	0.36	105	40.7	29	15	35	2.26	44
		3378	MN	2015	1	2	18	8	30.58	42.5055	-73.8255	0.00	0.6	1.6	0.42	105	13.4	32	21	36	2.19	53
		115719	MN	2015	1	28	17	43	14.62	43.7452	-74.1007	0.00	0.4	1.3	0.23	55	19.1	18	13	24	2.00	31
		115706	MN	2015	3	23	17	56	56.89	42.4972	-73.8353	0.00	0.7	1.7	0.26	207	14.0	21	8	24	2.25	29
		3337	MN	2015	3	24	19	40	6.99	43.7503	-74.0930	0.00	0.3	1.2	0.27	54	18.3	23	19	33	1.93	42
		115778	MN	2015	4	9	18	35	0.37	44.7862	-74.9983	2.93	0.5	1.6	0.26	140	35.3	13	14	17	2.17	27
		3327	MN	2015	4	14	15	10	4.30	42.9270	-74.9343	0.00	0.5	1.8	0.40	53	18.2	24	18	30	2.19	42
		3296	MN	2015	4	16	17	10	51.44	44.3000	-73.5847	0.00	0.4	1.4	0.25	47	39.3	21	13	24	1.89	34
		3414	MN	2015	4	21	16	8	5.49	44.3708	-74.1072	0.00	0.3	0.9	0.23	38	7.8	27	14	29	1.96	41
		3427	MN	2015	4	22	15	6	49.46	43.8212	-75.5432	0.00	0.5	1.6	0.27	89	16.0	16	10	19	1.76	26
		3390	MN	2015	4	22	16	37	9.16	42.9237	-74.1228	0.00	0.4	1.6	0.27	73	33.8	15	15	22	1.95	30
		115780	MN	2015	4	28	20	42	30.77	43.2673	-75.0902	0.00	0.4	1.0	0.17	85	47.9	18	11	20	1.92	29
		3520	MN	2015	5	18	15	13	55.05	44.0760	-75.8878	0.00	0.5	1.8	0.30	82	21.5	11	13	18	2.11	24
		3312	MN	2015	5	20	19	0	9.24	43.6277	-73.7872	0.00	0.6	2.6	0.45	85	19.9	21	14	28	2.36	35
		3318	MN	2015	5	26	15	1	51.10	43.8210	-76.1787	0.00	0.5	1.8	0.25	115	43.7	18	11	22	2.02	29
		3554	MN	2015	5	28	17	2	11.88	42.9185	-74.1118	0.00	0.4	1.5	0.28	73	38.2	21	14	25	1.88	35
		3359	MN	2015	6	1	17	50	21.04	44.7915	-74.9915	0.00	0.4	1.5	0.27	79	34.7	16	13	18	2.25	29
		3284	MN	2015	6	9	17	4	19.94	42.9842	-75.1863	0.00	0.4	1.5	0.31	67	42.5	23	18	29	2.27	41
		115708	MN	2015	6	12	16	12	38.73	45.1922	-73.6073	0.61	0.7	1.2	0.15	198	35.4	12	9	15	1.90	21
		3425	MN	2015	6	16	16	6	54.60	44.7737	-74.4455	0.00	0.3	1.0	0.23	81	8.8	12	17	20	1.75	29
		3448	MN	2015	6	24	16	37	32.09	42.6362	-74.2940	0.23	0.4	0.7	0.16	134	10.9	16	11	21	1.93	27
		3380	MN	2015	6	24	19	20	15.93	43.5323	-75.3132	0.00	0.4	1.7	0.31	60	19.2	24	13	29	2.20	37
		3551	MN	2015	7	10	17	59	56.43	43.3462	-73.5547	0.02	0.4	1.2	0.22	110	10.1	12	12	19	1.68	24
		3280	MN	2015	7	23	16	30	5.15	43.6305	-73.7820	0.00	0.4	1.6	0.26	85	19.8	22	13	26	2.43	35
		3382	MN	2015	7	30	16	14	24.26	44.3793	-74.0990	0.00	0.3	0.8	0.17	70	7.7	20	13	22	1.85	33
		3501	MN	2015	7	31	19	57	25.43	43.7283	-74.0813	0.00	0.7	2.6	0.36	92	18.3	16	10	18	1.63	26
		115712	MN	2015	9	16	16	52	28.34	42.9247	-74.1293	7.86	0.5	1.6	0.17	110	63.4	16	3	17	1.92	19
		314	MN	2015	10	21	17	17	20.32	42.9198	-74.1005	1.51	0.4	1.8	0.21	111	34.7	14	12	18	2.20	26
		309	MN	2015	11	3	16	4	29.36	43.8188	-75.5330	0.00	0.4	1.4	0.22	57	20.5	13	8	14	1.86	21
		317	MN	2015	11	20	17	25	37.02	42.9188	-74.1115	7.67	0.6	1.1	0.30	111	34.0	13	12	15	2.04	25
		307	MN	2016	1	15	20	27	47.35	42.4993	-73.8238	0.00	0.5	1.3	0.25	160	52.0	11	18	21	2.47	29
		315	MN	2016	2	11	19	15	13.43	42.5043	-73.8102	0.00	0.7	1.7	0.33	159	52.8	14	15	19	2.50	29
		313	MN	2016	2	23	21	9	4.17	42.4970	-73.8295	0.00	0.6	1.0	0.19	236	51.7	15	16	17	2.47	31
		319	MN	2016	3	8	18	10	45.55	42.4885	-73.8155	1.34	0.4	1.0	0.19	161	53.1	10	17	18	2.41	27
		301	MN	2016	3	16	16	41	2.92	42.6378	-74.2903	0.00	0.7	1.3	0.36	134	11.0	13	13	18	2.30	26
		321	MN	2016	3	23	17	10	18.45	43.7508	-75.4417	0.00	0.6	1.5	0.25	67	30.8	9	9	14	2.08	18
		302	MN	2016	4	7	17	0	11.42	43.6350	-73.7873	1.65	0.3	1.6	0.23	47	29.5	18	14	21	2.41	32
		3149	MN	2016	4	14	17	1	27.24	42.6480	-74.2893	3.53	0.5	1.0	0.28	133	10.4	15	15	20	2.39	30
		3065	MN	2016	5	19	15	7	23.32	42.9967	-75.2027	0.00	0.6	1.7	0.47	63	33.6	18	28	28	2.43	46
		3076	MN	2016	6	6	14	47	0.59	42.9203	-74.9568	0.00	0.5	1.6	0.41	81	55.7	14	20	22	2.16	34
		3077	MN	2016	6	14	18	31	2.72	43.6335	-73.7745	0.00	0.4	1.6	0.28	55	29.0	11	15	15	2.17	26
		3150	MN	2016	7	5	17	23	42.76	44.7877	-74.4532	4.03	0.5	0.9	0.15	128	7.2	8	7	10	1.91	15
		3130	MN	2016	7	14	14	48	40.15	42.9858	-75.2025	0.00	0.7	2.2	0.46	66	32.9	14	15	18	2.29	29
		3142	MN	2016	7	21	14	48	22.03	43.0135	-76.0623	0.00	0.8	2.5	0.55	43	44.3	11	21	22	1.54	32
		3093	MN	2016	8	3	18	0	23.73	43.6170	-73.7908	0.00	0.6	2.5	0.42	85	27.7	13	15	17	2.15	29
		3151	MN	2016	8	8	14	17	46.83	43.0082	-76.0692	0.00	1.0	2.8	0.53	60	45.0	8	17	19	1.74	25
		3114	MN	2016	8	12	15	31	0.10	44.7943	-74.4443	5.41	1.2	2.2	0.45	129	7.0	12	8	14	1.96	20
		3116	MN	2016	8	22	20	22	0.02	42.9858	-75.2005	0.00	0.8	2.4	0.53	66	33.0	11	22	24	2.28	33
		3108	MN	2016	9	19	14	17	15.33	43.8172	-75.5335	0.00	0.7	2.6	0.43	57	20.6	14	10	16	1.90	24

		3094	MN	2016	9	26	18	14	59.78	43.6232	-73.8072	0.00	0.9	3.2	0.68	57	28.8	12	18	21	2.11	30
		3109	MN	2016	9	27	15	47	11.37	43.3430	-73.5513	1.14	0.5	1.4	0.22	81	10.5	10	9	12	1.57	19
		3139	MN	2016	10	6	14	51	40.91	42.8950	-74.0892	7.00	0.8	1.1	0.30	190	64.3	12	17	19	1.97	29
		3095	MN	2016	10	6	17	54	7.28	43.7283	-74.1152	0.00	0.9	2.7	0.68	65	42.9	14	23	25	2.12	37
		3111	MN	2016	10	10	17	12	5.71	43.2710	-75.1085	0.00	0.6	1.7	0.49	64	17.4	16	23	24	2.41	39
		3141	MN	2016	10	13	16	41	48.06	43.3612	-73.5373	0.00	0.4	1.3	0.28	79	10.9	11	15	17	1.64	28
		3098	MN	2016	12	13	20	44	45.88	43.4915	-73.3985	0.00	0.5	1.9	0.40	72	24.8	15	21	22	2.07	36
		2421	MN	2017	2	3	16	15	42.36	44.3120	-73.5738	0.00	0.6	2.1	0.25	82	21.1	15	7	15	1.51	22
		2426	MN	2017	3	21	18	15	4.79	43.6247	-73.7765	0.00	0.4	1.5	0.27	47	28.1	15	15	19	2.08	30
		2457	MN	2017	3	24	16	22	49.07	43.7340	-74.0860	0.00	0.4	1.3	0.24	64	28.8	12	17	19	1.84	29
		2576	MN	2017	3	29	19	34	41.59	43.4843	-73.4177	5.47	0.7	3.4	0.35	71	23.1	14	21	23	1.90	36
		2486	MN	2017	3	30	15	38	46.30	43.8568	-75.9742	0.00	1.0	3.4	0.48	106	29.1	8	9	14	1.99	18
		2460	MN	2017	4	12	18	13	31.97	43.1335	-73.8980	0.09	0.5	1.4	0.32	95	33.5	15	21	23	1.94	36
		2492	MN	2017	4	14	16	48	0.49	43.8290	-76.1755	0.00	0.6	1.9	0.42	104	45.1	14	20	22	1.85	34
		2419	MN	2017	4	20	14	37	17.44	42.9862	-75.1877	0.00	0.5	1.4	0.37	67	33.9	17	24	25	2.43	41
		2569	MN	2017	5	4	16	24	18.82	42.9020	-73.2275	4.63	0.7	1.3	0.29	148	64.5	6	11	13	1.91	17
		2585	MN	2017	5	9	17	30	7.06	43.6390	-73.7485	0.00	0.8	2.8	0.45	87	29.0	13	12	16	2.05	27
		2497	MN	2017	5	12	16	5	4.62	43.8140	-75.5095	0.00	0.6	2.5	0.46	66	21.9	14	14	20	1.79	28
		2417	MN	2017	5	26	13	58	15.21	43.0050	-75.2217	0.00	0.7	1.7	0.46	72	39.8	14	24	24	2.49	38
		2462	MN	2017	6	2	17	2	55.58	43.6220	-73.7753	0.00	0.6	2.5	0.51	53	27.8	10	19	20	2.16	29

Column 1:

X - Event did not meet quality criteria

Notes - Quality criteria not met by an event

Z - Vertical error too high

H - Horizontal error too high

S - Too few stations after distance and RMS weighting in fourth iteration

Appendix Table A3 - Earthquake Locations and Errors

	Notes	ORID	Type	Time and Date						Location			Horz Error km	Vert Error km	RMS Err	Max Azimuth	Closest Station (km)	Number of Arrivals			Magnitude (ml)	# Mag Stations
				Year	Month	Day	Hour	Minute	Second	Latitude	Longitude	Depth km						P	S	# Stations		
	115665	EQ	2013	1	16	13	46	37.37	44.4983	-74.0743	9.94	0.3	0.7	0.15	71	53.70	13	12	14	1.83	25	
X ZH	115806	EQ	2013	2	16	7	44	36.05	42.6790	-74.0128	0.03	24.8	75.4	3.85	196	29.00	8	0	8	1.67	8	
	115807	EQ	2013	2	20	9	39	4.48	45.1105	-74.2017	6.50	0.5	1.4	0.19	155	38.50	10	11	12	1.75	21	
	2983	EQ	2013	2	26	10	31	34.60	44.8987	-74.5068	15.10	0.4	0.7	0.21	114	6.50	12	12	13	1.70	24	
	115808	EQ	2013	3	2	18	23	40.10	44.8113	-75.1932	11.47	0.7	1.5	0.20	114	52.90	4	7	8	1.55	11	
	115809	EQ	2013	3	7	23	12	5.72	42.5827	-74.1498	15.87	1.2	0.6	0.21	224	24.00	5	8	8	2.08	13	
	2985	EQ	2013	3	14	0	1	52.69	43.8202	-74.2142	7.96	0.2	0.7	0.11	107	17.10	10	10	11	1.94	20	
	115668	EQ	2013	3	17	21	34	39.43	43.8557	-74.0733	14.87	0.7	1.2	0.11	171	17.80	7	7	8	1.60	14	
	115669	EQ	2013	3	24	3	7	29.31	44.3005	-76.4997	1.76	0.5	1.7	0.27	115	37.70	11	13	16	1.48	24	
X Z	115670	EQ	2013	3	25	9	49	0.52	44.2802	-76.4905	3.12	0.3	13.8	0.13	111	39.30	11	9	13	1.52	20	
	115810	EQ	2013	4	1	11	28	4.04	44.0733	-76.0435	0.57	0.6	1.8	0.19	151	32.80	7	5	7	1.57	12	
X Z	115818	EQ	2013	5	2	1	54	5.90	44.7452	-74.9510	4.16	1.5	16.6	0.26	248	32.40	5	5	5	1.30	10	
	115672	EQ	2013	5	2	9	53	36.12	43.9065	-73.9575	14.96	0.7	2.1	0.07	236	22.60	3	4	5	0.86	7	
X Z	115819	EQ	2013	5	19	5	14	22.95	45.1985	-75.5125	3.16	0.3	18.6	0.20	59	28.70	16	14	17	1.46	30	
	115820	EQ	2013	6	16	5	47	23.30	45.2288	-75.3605	3.64	0.3	0.8	0.14	134	28.80	18	14	20	1.98	36	
X Z	115908	EQ	2013	7	20	23	5	6.98	44.9915	-74.5972	3.13	1.3	16.3	0.17	283	18.30	4	5	5	1.15	9	
	3002	EQ	2013	7	27	4	50	43.30	43.2857	-75.1072	5.26	0.4	0.7	0.12	118	87.30	10	5	13	1.80	15	
	115914	EQ	2013	8	18	19	4	52.85	45.2488	-74.0365	12.12	0.3	0.7	0.17	75	11.20	10	14	15	1.62	24	
	2987	EQ	2013	8	25	13	33	13.27	43.3395	-73.7568	4.87	0.6	0.8	0.32	176	79.90	25	21	29	2.54	46	
	2988	EQ	2013	8	27	4	40	14.19	44.6627	-74.0757	12.84	0.3	0.9	0.26	46	28.50	21	24	26	1.65	47	
	2990	EQ	2013	9	10	3	28	29.15	42.5927	-76.9095	6.37	0.3	0.9	0.20	56	35.70	19	25	32	1.60	44	
+	115742	EQ	2013	9	30	14	47	1.49	43.0522	-74.7000	8.82	1.0	3.0	0.31	110	48.50	13	5	16	1.81	18	
	2991	EQ	2013	11	10	2	32	21.87	44.9582	-74.8007	9.97	0.3	1.4	0.16	98	21.80	9	14	15	1.17	23	
+	3473	EQ	2013	12	3	18	30	3.91	43.0845	-73.8195	13.48	0.5	1.0	0.26	94	35.50	20	17	29	1.72	37	
	2992	EQ	2013	12	5	4	10	14.54	43.9970	-72.4510	5.99	0.5	1.7	0.21	127	20.80	14	10	17	1.78	24	
	3279	EQ	2013	12	21	15	21	14.63	45.1070	-74.0060	14.40	0.3	0.5	0.24	46	6.00	29	21	30	2.26	50	
X Z	115926	EQ	2014	1	3	2	10	48.75	44.7573	-75.1223	10.96	0.7	6.6	0.13	161	39.10	2	6	6	1.74	8	
	3353	EQ	2014	1	28	11	32	5.08	44.1118	-72.0843	7.87	0.8	1.3	0.39	193	22.30	24	16	27	2.34	40	
+	115744	EQ	2014	1	30	17	47	2.35	44.9257	-73.6053	6.26	0.7	1.7	0.22	132	10.20	8	7	10	1.40	15	
	3396	EQ	2014	2	2	4	55	35.33	43.9400	-72.0248	7.99	1.3	0.8	0.36	209	14.80	21	13	26	1.85	34	
	115822	EQ	2014	2	6	3	19	23.40	44.5733	-75.1193	1.48	0.4	1.7	0.17	98	24.80	7	10	11	1.53	17	
	3275	EQ	2014	2	7	15	45	6.07	45.0945	-73.6383	11.47	0.4	0.7	0.32	44	29.10	38	22	39	2.55	60	
	115823	EQ	2014	2	8	12	34	21.13	42.7007	-74.0887	13.76	0.3	0.6	0.20	94	18.90	13	19	21	1.28	32	
	115835	EQ	2014	2	23	2	19	8.59	44.7070	-73.8728	12.88	0.2	0.6	0.05	73	16.00	4	9	9	0.93	13	
	2995	EQ	2014	3	24	1	26	2.43	44.7620	-73.8197	11.80	0.2	0.5	0.12	44	16.50	20	20	23	1.57	40	
	2996	EQ	2014	4	1	21	26	39.63	44.5305	-75.9320	4.72	0.4	1.0	0.26	79	26.90	26	17	31	1.87	43	
	115838	EQ	2014	4	13	10	27	14.82	45.1897	-75.0132	21.67	4.5	1.5	0.49	261	9.80	4	3	6	1.19	7	
	2998	EQ	2014	4	17	15	14	21.56	43.1458	-73.9145	2.95	0.4	2.0	0.28	55	33.20	20	15	25	1.90	35	
	115678	EQ	2014	6	3	8	29	11.78	45.0157	-74.2073	11.42	0.4	1.6	0.05	168	19.10	5	6	6	0.81	11	
	2999	EQ	2014	6	5	20	49	43.30	44.8093	-75.9485	7.38	0.2	1.2	0.16	74	34.40	25	23	31	1.87	48	
X Z	115853	EQ	2014	6	17	14	39	29.28	43.9297	-75.6732	0.03	2.5	5.5	1.29	96	1.40	3	8	9	1.49	11	
	115957	EQ	2014	7	24	15	25	16.22	43.4117	-73.9750	10.62	0.4	1.9	0.36	70	25.10	13	28	28	1.51	19	
	3000	EQ	2014	8	1	6	18	30.61	43.8548	-72.3272	7.61	0.5	1.0	0.28	144	12.90	17	12	21	1.51	29	
	3260	EQ	2014	8	1	17	50	41.94	45.1268	-75.7182	10.82	0.2	0.8	0.18	70	57.70	29	22	35	2.25	51	
	115857	EQ	2014	8	4	20	50	3.78	44.1303	-73.0057	8.78	0.7	2.2	0.25	103	19.70	6	6	8	0.67	12	
+	3398	EQ	2014	8	20	15	6	50.13	43.9840	-72.4665	5.96	0.6	1.2	0.34	101	21.50	17	10	20	1.80	27	
	3001	EQ	2014	8	23	4	55	14.34	42.9317	-74.3938	4.87	0.4	1.3	0.29	42	26.10	30	19	37	1.89	49	
	115865	EQ	2014	9	16	12	36	18.24	45.0710	-74.2115	8.85	0.2	1.3	0.08	94	15.10	4	10	10	1.05	14	
	115873	EQ	2014	9	28	3	16	3.86	45.1488	-73.8713	12.48	0.2	0.7	0.10	81	14.40	8	11	13	1.06	19	
+	3483	EQ	2014	10	7	11	31	20.48	44.1172	-75.4525	0.03	0.5	1.5	0.34	79	22.20	20	23	30	1.65	43	
	115877	EQ	2014	11	13	3	30	7.79	43.6360	-73.9570	13.73	0.3	1.2	0.18	108	19.00	10	10	12	1.20	20	
	3004	EQ	2014	11	26	1	33	38.26	44.0998	-75.9742	0.04	0.4	1.2	0.20	102	28.80	15	11	21	1.80	26	

		115887	EQ	2014	12	23	11	39	57.37	44.0413	-74.1643	23.80	3.5	4.0	0.81	259	8.90	5	4	6	0.87	9
		3320	EQ	2014	12	30	2	44	50.15	45.1462	-74.2235	10.74	0.2	0.6	0.21	51	13.30	32	26	34	1.86	58
		115681	EQ	2015	1	11	15	54	57.39	44.6700	-73.6548	8.93	0.2	0.4	0.07	93	3.90	8	9	10	1.26	17
		3409	EQ	2015	1	19	16	35	14.29	45.1887	-74.1778	11.70	0.4	0.6	0.23	69	10.70	28	20	32	2.20	48
		115890	EQ	2015	1	19	19	39	10.96	45.1633	-74.2023	21.38	0.8	2.1	0.17	192	11.80	4	6	7	1.30	10
X	ZS	115953	EQ	2015	1	25	21	52	48.25	44.8617	-73.5268	13.76	1.3	5.7	0.01	176	36.60	2	3	5	1.75	3
		3005	EQ	2015	2	5	14	55	12.65	43.6768	-74.0742	8.94	0.2	1.2	0.06	138	20.80	10	9	12	1.46	19
		3006	EQ	2015	2	8	9	34	29.70	44.7655	-74.5933	8.73	0.3	1.3	0.11	78	16.20	10	10	12	1.31	20
		3007	EQ	2015	2	14	4	47	18.62	44.4555	-74.8105	14.75	0.6	1.2	0.22	132	25.70	9	10	14	1.67	19
		3008	EQ	2015	2	26	1	11	46.09	44.3270	-74.5260	7.44	0.3	1.3	0.21	55	29.40	18	17	22	1.63	35
		115891	EQ	2015	3	2	0	54	24.15	45.1258	-73.8498	12.37	0.3	0.8	0.08	97	16.30	9	12	13	1.19	21
+		3364	EQ	2015	3	23	20	48	37.36	42.9162	-74.1267	6.64	0.4	1.0	0.28	74	33.00	23	17	32	1.85	40
		3009	EQ	2015	4	8	14	27	17.51	44.0745	-75.2707	6.40	0.5	2.0	0.32	96	32.50	22	12	25	1.58	34
		3513	EQ	2015	4	17	0	53	47.94	45.1435	-73.8688	14.41	0.3	0.6	0.21	47	14.60	18	24	28	1.71	42
		3010	EQ	2015	5	8	1	47	16.80	44.7465	-75.1608	6.65	0.3	0.8	0.14	161	36.50	15	13	17	1.29	28
+		3518	EQ	2015	5	8	15	57	24.59	43.9727	-72.4705	10.62	0.4	1.9	0.26	116	21.50	17	13	22	1.94	
		3288	EQ	2015	5	23	20	21	58.80	45.0580	-74.2065	13.75	0.3	0.6	0.18	45	15.70	27	13	28	1.99	40
		115892	EQ	2015	5	23	20	21	58.78	45.0570	-74.1980	6.75	0.3	0.9	0.28	44	15.30	31	25	34	2.06	56
		115894	EQ	2015	5	25	7	17	43.38	43.6983	-74.0847	6.99	0.5	3.2	0.16	175	20.10	7	11	11	1.14	18
		115897	EQ	2015	6	1	8	31	28.70	44.0298	-75.1738	15.03	0.4	2.3	0.21	78	39.00	5	10	11	1.33	15
		115900	EQ	2015	7	13	19	27	27.72	45.1890	-73.9567	14.21	0.3	0.5	0.13	155	48.90	14	19	21	1.70	33
		115903	EQ	2015	7	27	15	25	8.35	44.5260	-73.7018	7.24	0.3	1.1	0.07	101	13.30	6	9	10	0.78	15
		115905	EQ	2015	8	2	3	46	48.62	44.4070	-72.3755	7.09	1.2	2.3	0.29	217	30.90	8	5	8	1.01	13
		3018	EQ	2015	9	27	3	16	23.20	42.4537	-74.4443	11.12	0.9	1.2	0.40	151	27.30	29	13	30	3.00	42
		328	EQ	2015	10	13	3	11	40.83	45.0645	-75.9427	15.59	0.7	1.8	0.22	166	104.00	8	11	11	1.51	21
		298	EQ	2015	10	28	20	42	14.81	43.0455	-74.3635	12.84	0.3	0.6	0.21	70	38.80	18	20	21	2.44	38
		330	EQ	2015	11	2	10	47	22.12	44.5610	-73.8822	14.57	0.3	1.2	0.11	94	38.30	9	9	11	1.33	18
X	Z	333	EQ	2015	11	3	7	16	55.69	43.4332	-76.6437	3.53	0.7	16.2	0.18	185	24.60	6	6	8	1.43	12
X	S	338	EQ	2015	11	4	11	1	13.14	44.9282	-73.7160	8.22	3.3	3.3	0.00	226	14.50	4	3	5	1.06	7
		304	EQ	2015	11	5	23	24	30.72	43.2560	-75.1707	18.00	0.4	1.0	0.21	69	14.90	16	14	18	1.71	30
		292	EQ	2015	11	28	5	16	53.83	44.9748	-74.7207	7.74	0.4	0.6	0.27	108	22.60	25	21	25	3.40	50
		324	EQ	2015	12	30	13	1	21.40	44.6102	-75.2430	6.50	0.5	1.2	0.24	115	51.70	10	11	15	2.06	22
		342	EQ	2016	3	9	1	39	21.26	45.0947	-74.0707	5.66	0.7	1.7	0.08	243	44.60	5	7	7	1.46	13
		344	EQ	2016	3	23	4	51	9.64	43.8615	-74.4543	7.70	0.5	1.0	0.10	169	22.40	5	5	5	1.41	10
		351	EQ	2016	4	4	0	48	33.89	45.1250	-75.1445	7.91	0.4	2.0	0.11	143	48.00	1	8	8	1.87	9
		354	EQ	2016	4	7	11	25	44.67	45.0728	-74.8568	6.20	0.4	0.8	0.13	155	37.90	6	10	10	1.57	18
		323	EQ	2016	4	10	6	14	48.68	44.9780	-74.1022	14.10	0.5	1.1	0.12	170	35.40	8	9	12	1.61	19
		3132	EQ	2016	4	12	3	10	58.03	44.9150	-73.8155	9.38	0.8	1.0	0.30	205	20.00	12	15	16	2.00	27
		3205	EQ	2016	4	13	8	50	36.19	44.9478	-73.5135	8.98	0.9	1.1	0.17	217	13.90	5	7	7	1.29	13
		3234	EQ	2016	4	16	9	40	42.33	43.8032	-74.7127	35.81	1.6	2.4	0.53	142	67.50	5	6	7	1.43	12
		3164	EQ	2016	4	28	9	45	21.92	44.4135	-74.9258	9.36	0.3	0.9	0.17	100	16.20	8	10	11	1.56	18
X	Z	3219	EQ	2016	5	4	11	5	27.72	43.0948	-72.1542	7.77	3.1	5.8	0.46	247	42.80	4	6	7	1.51	10
		3170	EQ	2016	5	19	8	15	43.25	43.9267	-75.7837	4.27	0.4	1.9	0.21	132	12.00	10	13	15	1.56	23
		3221	EQ	2016	5	22	0	28	53.85	44.1578	-75.5457	0.82	0.5	1.3	0.09	210	21.50	4	5	5	1.10	9
		3135	EQ	2016	6	5	2	5	17.93	44.5042	-73.6678	9.14	0.3	1.1	0.21	69	37.30	19	14	19	2.52	35
		3223	EQ	2016	6	14	6	25	16.00	44.8208	-74.0162	15.23	0.7	1.2	0.12	173	33.90	7	10	10	1.12	17
		3225	EQ	2016	6	18	4	15	43.29	44.9448	-73.5160	11.16	0.6	0.5	0.03	230	13.50	3	5	6	1.11	8
		3176	EQ	2016	6	29	3	13	50.04	44.3708	-75.3898	6.45	0.5	0.9	0.14	163	40.60	7	11	12	1.28	18
		3181	EQ	2016	7	10	13	22	23.09	44.8183	-74.5393	10.46	0.6	0.6	0.11	178	3.50	6	8	9	1.35	14
		3131	EQ	2016	8	20	8	50	23.73	43.5782	-76.6048	6.19	0.5	1.3	0.34	86	50.40	13	22	23	1.64	35
		3226	EQ	2016	8	27	18	36	45.70	45.2183	-74.3592	4.81	1.0	0.8	0.37	238	43.60	19	19	24	2.33	38
		3184	EQ	2016	9	25	4	40	17.21	45.0778	-74.1783	13.70	1.0	1.6	0.13	244	37.00	4	8	9	1.04	12
		3190	EQ	2016	10	8	21	10	48.18	44.8742	-74.4743	3.50	1.3	0.8	0.08	225	4.60	7	6	9	1.60	13
		3192	EQ	2016	10	20	19	1	11.30	45.0835	-74.0697	12.08	0.7	1.0	0.06	272	43.80	4	7	8	1.79	11

		3194	EQ	2016	10	30	23	38	39.94	44.7185	-73.8400	15.54	0.5	0.9	0.11	197	35.70	8	10	11	1.66	18
		3196	EQ	2016	12	25	8	38	44.08	44.2173	-72.9822	6.10	0.5	1.0	0.16	158	17.50	9	10	13	1.77	19
		2592	EQ	2017	1	1	18	21	45.57	43.2367	-73.0360	8.46	0.7	3.4	0.25	122	41.00	7	9	9	1.61	16
+		2574	EQ	2017	1	10	17	30	12.59	43.3057	-73.5705	0.02	0.3	1.0	0.21	83	11.80	11	12	16	1.68	24
		2456	EQ	2017	1	21	15	35	4.63	44.6343	-73.5783	14.33	0.4	0.9	0.26	80	22.30	12	19	19	1.75	31
		2629	EQ	2017	2	18	3	16	35.59	44.9410	-73.9312	12.29	0.5	1.6	0.08	210	29.50	5	9	9	1.79	14
		2416	EQ	2017	2	25	2	31	30.92	44.6177	-75.8028	1.12	0.7	1.6	0.42	169	68.00	25	29	31	2.07	54
		2575	EQ	2017	3	12	16	49	21.83	44.6733	-74.5113	5.19	0.3	0.6	0.13	111	8.20	7	14	15	1.96	22
		2605	EQ	2017	4	25	11	48	3.44	44.6727	-74.5758	6.94	0.5	4.1	0.14	129	19.40	6	7	8	1.20	15
		2537	EQ	2017	4	29	6	55	25.29	43.7218	-73.2875	1.50	0.3	1.6	0.20	82	35.10	10	16	17	1.45	26
		2577	EQ	2017	5	13	19	4	11.06	43.8772	-73.2673	11.68	0.3	1.3	0.11	143	23.70	10	14	15	1.51	24
		2418	EQ	2017	6	1	7	22	44.48	43.7317	-73.2997	6.27	0.3	1.3	0.23	80	35.00	15	18	19	1.61	33

Column 1:

X - Event did not meet quality criteria

+ - Earthquakes was not listed in the ANSS catalog

Notes - Quality criteria not met by an event

Z - Vertical error too high

H - Horizontal error too high

S - Too few stations after distance and RMS weighting in fourth iteration

Appendix Table A4 - Earthquake Locations and Errors from the ANSS Catalog

	Corresponding ORID	Time and Date						Location			Horz Error km	Vert Error km	RMS Err	Max Azimuth	Closest Station (km)	Number of Arrivals			Magnitude (ml)	# Mag Stations
		Year	Month	Day	Hour	Minute	Second	Latitude	Longitude	Depth km						P	S	# Stations		
	115665	2013	1	16	13	46	37.77	44.4932	-74.0662	5.00	0.40	31.61	0.17	54	53.69			12	2.16	17
X	115806	2013	2	16	7	44	25.59	43.0795	-74.1000	6.40	0.38	1.41	0.08	100	48.81			8	1.33	10
	115807	2013	2	20	9	39	4.81	45.0995	-74.2070	4.90	0.38	31.61	0.20	153	37.32			12	1.93	9
	2983	2013	2	26	10	31	35.07	44.8950	-74.5235	12.53	0.42	0.80	0.21	65	6.28			11	1.80	14
	115808	2013	3	2	18	23	39.03	44.8123	-75.2677	18.90	1.09	1.90	0.12	222	20.91			5	1.41	6
	115809	2013	3	7	23	12	6.11	42.5920	-74.1458	15.35	0.22	0.53	0.12	105	23.77			12	1.46	5
	2985	2013	3	14	0	1	53.30	43.8283	-74.2360	5.00	0.53	31.61	0.25	92	16.16			14	2.16	17
	115668	2013	3	17	21	34	39.89	43.8340	-74.1003	12.83	0.56	1.52	0.24	134	18.36			10	1.29	6
	115669	2013	3	24	3	7	29.21	44.2877	-76.4832	1.00	0.57	31.61	0.34	108	38.34			15	1.85	9
X	115670	2013	3	25	9	49	0.67	44.2825	-76.4807	1.00	0.62	31.61	0.32	111	38.76			12	1.73	9
	115810	2013	4	1	11	28	4.61	44.0688	-76.0213	7.52	0.85	6.58	0.26	152	30.97			6	1.54	10
X	115818	2013	5	2	1	54	5.30	44.7482	-74.9807	8.22	0.39	0.80	0.07	151	9.44			7	0.33	4
	115672	2013	5	2	9	53	37.05	43.9087	-73.9885	7.16	0.47	3.35	0.24	80	20.15			12	0.77	5
X	115819	2013	5	19	5	14	23.25	45.2082	-75.5182	4.98	0.30	1.79	0.19	58				16	1.62	15
	115820	2013	6	16	5	47	23.57	45.2440	-75.3580	5.00	0.31	31.61	0.16	87				19	2.05	34
X	115908	2013	7	20	23	5	7.19	44.9832	-74.6032	4.10	1.07	9.82	0.12	284	17.67			4	0.52	2
	3002	2013	7	27	4	50	44.17	43.3038	-75.0882	5.00	0.42	31.61	0.31	47	87.86			24	1.80	25
	115914	2013	8	18	19	4	53.59	45.2362	-74.0250	9.46	0.60	1.58	0.37	84				11	1.54	13
	2987	2013	8	25	13	33	14.14	43.3510	-73.7943	10.17	0.45	0.99	0.33	60	10.91			23	2.46	31
	2988	2013	8	27	4	40	14.42	44.6673	-74.0823	13.85	0.31	1.48	0.22	64	38.70			15	1.84	7
	2990	2013	9	10	3	28	29.40	42.5963	-76.9065	5.00	0.29	31.61	0.35	33	35.35			39	1.69	44
+	115742																			
	2991	2013	11	10	2	32	22.25	44.9553	-74.8060	5.00	0.50	31.61	0.27	109	21.73			11	1.62	8
+	3473																			
	2992	2013	12	5	4	10	14.99	44.0092	-72.4587	5.24	0.55	10.83	0.19	105	36.53			8	1.69	4
	3279	2013	12	21	15	21	15.17	45.1142	-74.0120	10.80	0.36	0.84	0.37	75				32	2.16	53
X	115926	2014	1	3	2	10	49.08	44.7717	-75.1153	5.24	0.81	14.52	0.25	162	38.31			4	1.92	2
	3353	2014	1	28	11	32	4.78	44.1225	-72.0223	3.83	0.71	3.78	0.59	40				25	2.21	37
+	115744																			
	3396	2014	2	2	4	55	35.23	43.9480	-72.0013	5.00	0.38	31.61	0.50	36				38	1.86	93
	115822	2014	2	6	3	19	23.65	44.5608	-75.1253	7.51	0.47	2.17	0.25	74	16.61			16	1.70	12
	3275	2014	2	7	15	45	6.51	45.0958	-73.6460	12.00	0.33	31.61	0.38	60				44	2.42	23
	115823	2014	2	8	12	34	21.52	42.6930	-74.0897	11.92	0.30	1.30	0.26	38				24	1.38	23
	115835	2014	2	23	2	19	9.07	44.7115	-73.8730	9.40	0.37	2.03	0.26	74	16.24			15	1.25	9
	2995	2014	3	24	1	26	2.96	44.7683	-73.8277	5.00	0.38	31.61	0.29	77	17.46			18	1.64	19
	2996	2014	4	1	21	26	39.78	44.5102	-75.9473	4.17	0.35	31.61	0.28	113	26.47			23	1.89	25
	115838	2014	4	13	10	27	15.29	44.9763	-74.8253	9.41	0.99	2.10	0.17	135	18.97			6	0.51	7
	2998	2014	4	17	15	14	21.44	43.1327	-73.9198	0.01	0.67	31.61	0.36	57	34.66			16	1.93	5
	115678	2014	6	3	8	29	12.28	45.0135	-74.1998	8.73	0.36	31.61	0.23	74	18.97			16	0.49	14
	2999	2014	6	5	20	49	43.56	44.8177	-75.9717	12.10	0.41	1.17	0.23	123	33.83			24	2.09	28
X	115853	2014	6	17	14	49	9.20	45.1167	-74.2522	4.10	1.39	17.71	0.27	210	36.74			6	1.13	5
	115957	2014	7	24	15	25	16.80	43.4063	-73.9892	7.00	0.43	31.61	0.31	69	26.17			22	1.22	22
	3000	2014	8	1	6	18	31.19	43.8658	-72.3263	5.00	0.31	31.61	0.33	43				30	1.50	29
	3260	2014	8	1	17	50	42.26	45.1378	-75.7252	7.62	0.33	2.31	0.22	120	28.51			22	2.21	62
	115857	2014	8	4	20	50	4.32	44.1300	-73.0158	7.97	0.34	1.57	0.16	93	19.68			17	0.48	9
+	3398																			
	3001	2014	8	23	4	55	14.76	42.9395	-74.4312	5.00	0.39	31.61	0.35	39				29	2.08	30
	115865	2014	9	16	12	36	18.75	45.0733	-74.2345	7.37	1.51	12.41	0.39	149	33.69			7	1.17	6
	115873	2014	9	28	3	16	4.23	45.1603	-73.8660	10.11	0.85	2.25	0.29	185	14.85			11	0.49	14



	3181	2016	7	10	13	22	23.22	44.8233	-74.5392	10.47	0.44	0.71	0.21	125	3.17			9	1.15	9
	3131	2016	8	20	8	50	23.58	43.5658	-76.6178	5.00	0.51	31.61	0.28	72	37.63			15	1.48	13
	3226	2016	8	27	18	36	45.50	45.2483	-74.3473	11.92	0.70	1.41	0.18	227	47.13			10	1.73	14
	3184	2016	9	25	4	40	17.90	45.0803	-74.1725	5.28	1.07	31.61	0.42	153	37.55			11	0.71	10
	3190	2016	10	8	21	10	47.74	44.9108	-74.5133	5.00	0.88	31.61	0.25	119	7.91			11	1.23	5
	3192	2016	10	20	19	1	11.08	45.0988	-74.0242	5.29	0.81	12.66	0.20	184	47.74			9	1.01	6
	3194	2016	10	30	23	38	40.64	44.7010	-73.8683	15.92	0.77	3.25	0.34	133	33.99			12	0.97	10
	3196	2016	12	25	8	38	43.70	44.2048	-73.0289	1.71	1.50	3.30	0.38	87	25.58				1.80	14
	2592	2017	1	1	18	21	44.69	43.2067	-73.0534	5.00	1.30	2.00	0.57	106	43.37				1.60	16
+	2574																			
	2456	2017	1	21	15	35	5.07	44.6333	-73.6032	13.99	0.37	1.48	0.26	74	22.45			15	1.72	19
	2629	2017	2	18	3	16	35.13	44.9642	-73.9165	18.94	0.74	1.19	0.13	215	29.65			9	0.65	7
	2416	2017	2	25	2	31	31.06	44.6175	-75.8178	5.00	0.72	31.61	0.24	204	69.21			19	1.87	13
	2575	2017	3	12	16	49	22.10	44.6768	-74.5295	5.00	0.32	31.61	0.19	97	7.64			15	1.33	14
	2605	2017	4	25	11	48	3.46	44.6747	-74.5790	9.13	0.42	2.38	0.15	101	19.25			10	0.98	9
	2537	2017	4	29	6	55	25.79	43.7193	-73.3067	7.48	0.43	5.73	0.21	96	36.34			16	1.32	19
	2577	2017	5	13	19	4	11.34	43.8700	-73.2647	12.74	0.36	1.74	0.13	146	23.82			12	1.32	15
	2418	2017	6	1	7	22	44.99	43.7362	-73.3372	4.15	0.29	31.61	0.18	70	36.84			19	1.34	25

Appendix Table A5 - Comparison of Earthquake Locations and Errors in this Study and the ANSS Catalog  
 (Negative values indicate the value is smaller in this study.)

	ORID	# Stations	Vert. Error	Horz. Error	RMS	Azimuth Cap	Closest Station km	#Mag Station	Magnitude	Distance (km)
	115665	2	-30.91	-0.10	-0.33	17	0.01	8	-0.33	0.87
X	115806	0	73.99	24.42	3.41	96	-19.81	-2	0.34	45.10
	115807	0	-30.21	0.12	-0.15	2	1.18	12	-0.18	1.29
	2983	2	-0.10	-0.02	0.15	49	0.22	10	-0.10	1.37
	115808	3	-0.40	-0.39	0.01	-108	31.99	5	0.14	5.88
	115809	-4	0.07	0.98	0.00	119	0.23	8	0.62	1.09
	2985	-3	-30.91	-0.33	-0.04	15	0.94	3	-0.22	1.97
	115668	-2	-0.32	0.14	-0.06	37	-0.56	8	0.31	3.24
	115669	1	-29.91	-0.07	-0.07	7	-0.64	15	-0.37	1.94
X	115670	1	-17.81	-0.32	-0.22	0	0.54	11	-0.21	0.82
	115810	1	-4.78	-0.25	-0.09	-1	1.83	2	0.03	1.84
X	115818	-2	15.80	1.11	0.18	97	22.96	6	0.97	2.37
	115672	-7	-1.25	0.23	-0.11	156	2.45	2	0.09	2.50
X	115819	1	16.81	0.00	0.20	1	28.70	15	-0.16	1.16
	115820	1	-30.81	-0.01	0.14	47	28.80	2	-0.07	1.70
X	115908	1	6.48	0.23	0.01	-1	0.63	7	0.63	1.04
	3002	-11	-30.91	-0.02	-0.67	71	-0.56	-10	0.00	2.54
	115914	4	-0.88	-0.30	0.17	-9	11.20	11	0.08	1.67
	2987	6	-0.19	0.15	0.22	116	68.99	15	0.08	3.29
	2988	11	-0.58	-0.01	-0.09	-18	-10.20	40	-0.19	0.74
	2990	-7	-30.71	0.01	-0.12	23	0.35	0	-0.09	0.48
+	115742									
	2991	4	-30.21	-0.20	-0.04	-11	0.07	15	-0.45	0.52
+	3473									
	2992	9	-9.13	-0.05	-0.12	22	-15.73	20	0.09	1.49
	3279	-2	-0.34	-0.06	0.24	-29	6.00	-3	0.10	0.93
X	115926	2	-7.92	-0.11	-0.21	-1	0.79	6	-0.18	1.69
	3353	2	-2.48	0.09	0.39	153	22.30	3	0.13	5.09
+	115744									
	3396	-12	-30.81	0.92	0.36	173	14.80	-59	-0.01	2.08
	115822	-5	-0.47	-0.07	0.02	24	8.19	5	-0.17	1.47
	3275	-5	-30.91	0.07	0.32	-16	29.10	37	0.13	0.62
	115823	-3	-0.70	0.00	0.20	56	18.90	9	-0.10	0.86
	115835	-6	-1.43	-0.17	-0.10	-1	-0.24	4	-0.32	0.50
	2995	5	-31.11	-0.18	-0.04	-33	-0.96	21	-0.07	0.95
	2996	8	-30.61	0.05	0.02	-34	0.43	18	-0.02	2.57
	115838	0	-0.60	3.51	0.32	126	-9.17	0	0.68	27.93
	2998	9	-29.61	-0.27	-0.03	-2	-1.46	30	-0.03	1.53

	115678	-10	-30.01	0.04	-0.12	94	0.13	-3	0.32	0.64
	2999	7	0.03	-0.21	-0.14	-49	0.57	20	-0.22	2.05
X	115853	3	-12.21	1.11	0.96	-114	-35.34	6	0.36	173.52
	115957	6	-29.71	-0.03	0.12	1	-1.07	-3	0.29	1.29
	3000	-9	-30.61	0.19	0.28	101	12.90	0	0.01	1.23
	3260	13	-1.51	-0.13	-0.08	-50	29.19	-11	0.04	1.34
	115857	-9	0.63	0.36	0.07	10	0.02	3	0.19	0.81
+	3398									
	3001	8	-30.31	0.01	0.29	3	26.10	19	-0.19	3.16
	115865	3	-11.11	-1.31	-0.22	-55	-18.59	8	-0.12	1.82
	115873	2	-1.55	-0.65	-0.03	-104	-0.45	5	0.57	1.35
+	3483									
	115877	-13	-1.45	0.06	0.00	41	-1.19	3	-0.02	1.47
	3004	7	-30.41	-0.29	-0.09	-13	-3.31	12	-0.04	4.15
	115887	-4	3.45	3.04	0.76	195	2.89	-5	0.25	11.53
	3320	14	-1.04	-0.30	0.21	-43	13.30	28	-0.06	0.99
	115681	-12	-0.58	-0.17	0.03	45	-0.52	9	-0.34	0.91
	3409	2	-31.01	-0.04	0.12	-83	-1.22	18	0.08	1.95
	115890	-5	0.53	0.15	0.07	51	0.39	2	0.03	4.48
X	115953	-1	-2.98	0.52	-0.16	-51	17.66	1	1.50	153.89
	3005	-9	-30.41	-0.12	-0.14	73	-1.01	-11	-0.30	1.02
	3006	-4	-2.44	-0.10	-0.04	-5	-0.28	6	-0.06	0.40
	3007	-6	-30.41	0.16	-0.02	53	-1.13	4	-0.03	1.19
	3008	0	-30.31	-0.12	-0.06	0	-0.29	7	-0.19	0.35
	115891	1	-0.63	-0.37	-0.08	-83	-1.64	1	0.02	3.27
+	3364									
	3009	2	-0.96	-0.01	0.05	-4	1.94	10	-0.22	2.08
	3513	5	-0.55	0.00	0.08	-34	0.24	30	-0.11	0.40
	3010	-2	-30.81	-0.07	-0.01	29	19.32	1	-0.23	0.46
+	3518									
	3288	2	-0.99	-0.09	0.03	-36	-0.81	21	-0.10	0.79
	115892	26	-0.32	-0.32	0.14	-56	-0.82	50	-0.02	3.91
	115894	-2	-28.41	0.02	-0.03	74	-1.05	0	0.61	1.52
	115897	-2	-1.32	0.00	-0.14	3	0.11	3	0.87	2.10
	115900	5	-1.79	-0.16	-0.26	64	5.31	5	-0.24	0.19
	115903	-5	-1.43	-0.02	-0.05	29	0.47	-3	-0.26	1.93
	115905	8	0.30	-0.50	0.05	141	4.10	1	-0.39	6.54
	3018	8	0.39	0.52	0.14	108	-1.12	10	0.21	1.36
	328	-3	-1.19	-0.35	-0.16	1	61.98	11	-0.03	3.05
	298	-9	-3.58	-0.06	-0.14	38	-0.48	24	0.10	1.29

	330	-1	-1.75	-0.10	-0.23	-3	0.21	9	0.22	1.61
X	333	-2	-15.41	-0.38	-0.02	108	2.26	5	0.33	2.43
X	338	-4	-28.31	2.07	-0.12	67	0.61	1	0.85	0.58
	304	-4	0.08	-0.06	0.07	18	-0.93	1	0.01	1.34
	292	1	-31.01	-0.01	0.06	44	-0.87	-1	0.17	0.87
	324	6	-9.91	-0.04	-0.16	-61	7.00	14	0.45	1.36
	342	1	-8.68	-0.76	-0.33	32	-0.93	11	0.81	1.64
	344	-4	-30.61	-0.48	-0.11	74	-1.37	2	0.93	1.71
	351	0	-0.17	-0.40	-0.06	-107	28.93	4	1.44	1.93
	354	0	-5.63	-0.35	-0.18	-10	3.05	10	0.47	0.98
	323	-5	-6.20	-0.15	-0.19	51	0.52	8	0.48	1.15
	3132	-2	-30.61	0.14	0.10	106	-1.82	10	0.21	2.16
	3205	-1	-30.51	0.03	0.02	-4	-2.32	7	0.72	3.04
	3234	-4	-40.20	-0.01	0.36	70	48.13	4	0.39	24.57
	3164	-2	-2.78	-0.19	0.02	-6	-0.51	8	0.13	0.56
X	3219	7	1.70	1.70	0.05	155	-2.68	-8	-0.09	4.81
	3170	1	-29.71	-0.38	0.10	0	-0.14	11	0.18	1.26
	3221	-1	-12.02	-0.65	-0.13	-5	-2.70	4	0.62	2.86
	3135	-5	-30.51	-0.17	-0.12	30	0.35	13	0.28	1.74
	3223	0	-0.93	-0.28	-0.19	-11	-0.48	10	0.02	3.52
	3225	-2	-1.37	-0.18	-0.10	13	-0.69	1	0.56	0.99
	3176	0	-6.25	-0.03	-0.18	46	4.84	7	0.15	0.88
	3181	0	-0.11	0.16	0.08	53	0.33	5	0.20	0.56
	3131	8	-30.31	-0.01	0.00	14	12.77	22	0.16	1.73
	3226	14	-0.61	0.30	-0.05	11	-3.53	24	0.60	3.46
	3184	-2	-30.01	-0.07	-0.21	91	-0.55	2	0.33	0.54
	3190	-2	-30.81	0.42	0.01	106	-3.31	8	0.37	5.11
	3192	-1	-11.66	-0.11	-0.37	88	-3.94	5	0.78	3.96
	3194	-1	-2.35	-0.27	-0.20	64	1.71	8	0.69	2.97
	3196	13	-2.30	-1.00	-0.07	71	-8.08	5	-0.03	3.98
	2592	9	1.40	-0.60	-0.14	16	-2.37	0	0.01	3.62
+	2574									
	2456	4	-0.58	0.03	0.06	6	-0.15	12	0.03	1.97
	2629	0	0.41	-0.24	-0.19	-5	-0.15	7	1.14	2.82
	2416	12	-30.01	-0.02	-0.20	-35	-1.21	41	0.20	1.19
	2575	0	-31.01	-0.02	0.06	14	0.56	8	0.63	1.49
	2605	-2	1.72	0.08	-0.03	28	0.15	6	0.22	0.33
	2537	1	-4.13	-0.13	-0.13	-14	-1.24	7	0.13	1.57
	2577	3	-0.44	-0.06	-0.10	-3	-0.12	9	0.19	0.83
	2418	0	-30.31	0.01	-0.10	10	-1.84	8	0.27	3.05